CFD SIMULATION OF TWO PHASE FLOW AND HYDRATE PREDICTION IN A PIPELINE

By

KUM CHEE YAN

FINAL YEAR REPORT

Submitted to the Mechanical Engineering Programme
in Partial Fulfillment of the Requirements
Bachelor of Engineering (Hons)
(Mechanical Engineering)

JUNE 2009

Universiti Teknologi Petronas
Bandar Seri Iskandar
31750 Tronoh
Perak Darul Ridzuan

CERTIFICATION OF APPROVAL

CFD SIMULATION OF TWO PHASE FLOW
AND HYDRATE PREDICTION
IN A PIPELINE

By

KUM CHEE YAN
8727

A project dissertation submitted to the
Mechanical Engineering Programme
Universiti Teknologi PETRONAS
In partial fulfillment of the requirement for the
BACHELOR OF ENGINEERING (Hons)
(MECHANICAL ENGINEERING)

JUNE 2009

Approved by,

_____

(DR AHMED MAHER SAID ALI)

Project Supervisor

Universiti Teknologi Petronas
Bandar Seri Iskandar
31750 Tronoh
Perak Darul Ridzuan

CERTIFICATION OF ORIGINALITY

This is to certify that I am responsible for the work submitted in this project, that the original work is my own except as specified in the references and acknowledgements, and that the original work contained herein has not been undertaken or done by unspecified sources or persons.

_____

(KUM CHEE YAN)

ABSTRACT

Pipeline-risers systems are frequently encountered in the petroleum industry especially in the offshore platforms. It is also a common feature that in oil and gas production and transportation to have an existing multiphase flow. However due to the presence of more than one phase in the system, an analysis of the physical properties of such a fluid flow is difficult. In the case of two-phase flows in pipelines, flooding of the separation facilities could be expected due to the generation of severe slugs at the bottom of the riser. The size and frequency of the slugs are functions of the accumulation and displacement of liquid at the base of the riser. They can be controlled with an adequate model. Due to this phenomenon, significant advances have been made towards using computational fluid dynamics methods (CFD) to model the pressure gradient of two-phase flows in pipelines. The aim of this research project is to apply CFD methods to determine the pressure gradient in two phase flow pipelines and to simulate severe slugging phenomenon in pipeline- riser system using various empirical correlations methods. The results are compared with previous mathematical models where the possibility of hydrates formation is determined. Due to unavailability of experiment data, further validation of results cannot be achieved. The model can be used to design new pipeline riser-system or to adjust the operation of existing systems to prevent the occurrence of severe slug flow.

Keywords: Gas-liquid; Two-phase flow; CFD modeling

ACKNOWLEDGEMENT

The author would like to take the opportunity of prefacing the report in the best possible manner, by acknowledging all parties who had helped making the author's Final Year Project an educational yet a meaningful one.

In completing this project, the author would like to express his utmost gratitude to Dr Ahmed Maher Said Ali of Mechanical Engineering Department, Universiti Teknologi PETRONAS (UTP), who was the supervisor of the project, for his guidance, advice, help and experience. It was his guidance that a topic that was so alien to the author became familiar and interesting.

The author is ever grateful to a multitude of persons he has come across who have shown the way in tacking this project. The author would like to thank Mr. Suren Lim Sinnadurai for his assistance, kindness and overwhelming support especially in conveying details about his experience and expertise in using FLUENT and assisting the author in navigating the new software. A great thank you is also in order to Mr Gunawan for his experience in dealing with the software allows the sorting out of all types of misdirection taken by the author during the simulation phase.

Finally, the author would like to thank all the people who have been directly and indirectly involved in the completion of the project, especially those from UTP.

TABLE OF CONTENTS

LIST OF TABLES

LIST OF FIGURES

NOMENCLATURE

A	cross sectional area of pipe (m)
d	internal diameter of pipe (m)
f	friction factor
F	body forces
g	gravity (m^2/s)
k	kinetic energy
Re	Reynolds Number
P	Perimeter of pipe (m)
p	pressure (N/m^2)
u	velocity (m/s)

Greek symbols

α	volume fraction
ε	dissipation of kinetic energy
γ	normal distance from wall at the cell center
μ	viscosity (kg/ms)
ρ	density of fluid (kg/m*3*)
τ	shear stress (Pa)

Subscripts

0	inlet conditions
c	continuous phase
d	dispersed phase
i	interphase
g	gas phase
l	liquid phase
s	superficial
w	wall conditions

CHAPTER 1
INTRODUCTION

1.1 Background of Study

When two or more phases flow simultaneously in pipes, the flow behavior is much more complex that for single-phase flow. The phases tend to separate because of differences in density. Shear stresses at the pipe wall are different for each phase as a result of their difference densities and viscosities. Expansion of the highly compressible gas phase with decreasing pressure increases the in-situ volumetric flow rate of the gas. As a result, the gas and liquid do not travel at the same velocity in the pipe. For upward flow, the less dense, more compressible, less viscous gas phase tends to flow at a higher velocity than the liquid phase, causing a phenomenon known as slippage. However, for downward flow, the liquid often flows faster than the gas.

In pipeline flows, the pressure gradient in the flow direction is of great importance, as it gives engineers an idea of the pressure drop in the fluid as it travels along the pipeline. This is of crucial importance in two phase flows, as the fluid behavior of one or both the phases may change with pressure. For example, the density of the gas phase may be pressure dependant, or hydrate formation may occur at a particular pressure and temperature.

The blockage of the risers and pipelines of oil causes loss economical profit for oil companies. One of the main blockages is caused by the hydrate that forms due to temperature and pressure variation. Ideally, a pipeline would produce a constant amount of gas and liquid. In a single pipeline, however, segregated flow of liquid and gas may cause problems. The actual velocity of the gas phase is faster than the actual liquid velocity. The liquid phase has the tendency to accumulate in the dips and inclined pipe sections causing irregular flow behavior. As a result, large volumes of liquid may flow through the pipeline. These plugs of liquid are called slugs, or riser-induced slugging, and hydrodynamic slugs. Furthermore, operational changes, such

as start-up and production increase, can create large liquid slugs. Liquid slugs at the outlet of pipelines or riser systems may result in large oil and gas production losses. Production deferment results from poor use of downstream separators, process instabilities, time-consuming start-ups and, especially for flowline/riser systems, topside choking to avoid slugging. The transportation of a slug requires a larger pressure behind the slug to keep the plug moving through the pipeline. This pressure increase depends on the size of the liquid slug. After the slug arrives at the outlet of the pipeline or production platform, the compressed gas creates a large gas surge, which again may result in major upsets in topside facilities.

1.2 Problem Statement

Hydrates are of utmost importance in deepwater oil or gas well because ambient temperatures are low enough to be in the hydrate formation at operating pressure. The presence of certain amount of water in the hydrocarbon systems can be troublesome due to the formation of hydrates. Therefore, hydrate formation due to change of temperature and pressure during extracting oil causes blockage and production loss in risers. Hydrate crystals can develop into flow blockages which can be time-consuming to clear and cause safety problems. Lost or delayed revenue and costs associated with hydrates blockages can be significant due to vessel intervention cost and delayed production. Understanding the possible zones of hydrate formation is useful as to introduce ways to prevent them. Therefore, there is also a need for a mathematical model to simulate the hydrates forming conditions. This mathematical model is in the form of empirical correlations.

1.3 Objectives

The following are the main objectives of the project:

- To study the behavior of the multiphase flow during gas production from a gas well.
- To understand the conditions of possible hydrate formation inside the riser such as flow assurance.
- To simulate the multiphase flow inside a riser using CFD modeling.
- To predict hydrates locations on different empirical correlations

1.4 Scope of Study

In this project, the scope of studies includes the study of the behavior of multi-phase flow in the riser of a deep oil well where it is use for transportation. The formation of hydrates due to certain temperature and pressure could block the transport pipeline. Therefore, the author's focus is on gas hydrates formation in three phase equilibrium such as liquid water, hydrocarbon gas and solid hydrate. Other than that, it is a study of using correlations to predict the gas-hydrates formation at a given temperature or when pressure is available. All of the result will be simulated in the multiphase flow using CFD modeling such as Fluent.

1.5 Significance of Work

This project will provide the understanding of the multiphase flow where the flow consists of different phases which travel together at different velocity due to different in phase properties such as density.

Hydrates formation is a well known problem in the oil and gas industry and cost millions of dollars in production and transmission pipelines. The hydrates formation is getting harder to predict especially in deep oil well where the pressure and temperature varies according to depth.

With the simulation of the flow, it can help to forecast hydrates formation condition for most systems of hydrate formers and therefore leads to design remediation scheme.

CHAPTER 2
LITERATURE REVIEW AND THEORY

2.1 Multiphase Flow

There are many approaches that have been applied to date in the study of the modeling of multiphase. The true predictions of fluid flow are only available for single-phase laminar flows and very low Reynolds number flows in simplified geometries. However, when the Reynolds number increases to values typical of real applications, the true predictions are no longer available and the only practical way forward is through empiricism. Therefore, multiphase flows with deformable interfaces are able to take a virtually infinite number of configurations which will present an intractable problem which only in much idealized scenarios. For example laminar flow over an isolated spherical particle, bubble or droplet, yield analytical solutions to the conservation equations. This is particulate true given that in the vast majority of cases multiphase flows are turbulent in nature. Thus, the analysis and modeling of multiphase flows relies heavily on empiricism and the predictions for the models are only as reliable as the empirical relationships on which they are based [1].

Numerous visualization experiments have been performed over the last fifty years and it was natural that flow patterns or flow regimes to be defined and for flows to be categorized accordingly. Hewitt [2] provides an introductory discussion of flow patterns and states that these can themselves be categorized into three types which are dispersed, separated and intermittent flows. [3] Dispersed flows include all flow regimes where one phase is uniformly distributed as roughly spherical elements throughout another continuous phase. Such flows include bubbly flow where small gas bubbles are dispersed through a liquid continuous phase or drop flow where small droplets of liquid are carried along in a vapor stream. Separated flows are those where the phases are not intimately mixed. These include stratified flow in horizontal pipes where the liquid flows at the base of the pipe with a gas stream flowing above,

and annular flow where the liquid flows around the periphery of the pipe as a thin film with a gas core flowing internally. Finally, intermittent flows include those where the phases are not distributed uniformly along the pipe, for example slug flow or plug flow. Slug flow creates tremendous turbulence at the front of the slug. At the slug front, gas bubbles are entrained in the liquid. They impact and collapse on the pipe wall, resulting in instantaneous high shear. Therefore, slug flow generates a very high shear stress at the pipe wall which will tend to corrode the pipe [4].

Figure 1 presents an illustration of the various flow patterns that exist in vertical two-phase flows. At lower gas-liquid ratios, the fluids flow as a bubbly flow with small bubbles of gas distributed throughout the continuous liquid phase (which in oil and gas production is probably itself a water-in-oil dispersion). At higher gas-liquid ratios, the fluids are transported in the annular flow regime. For intermediate gas-oil ratios the slug and churn flow regimes occur and, at high flow rates of liquid and gas, the wispy annular flow regime occurs [5].

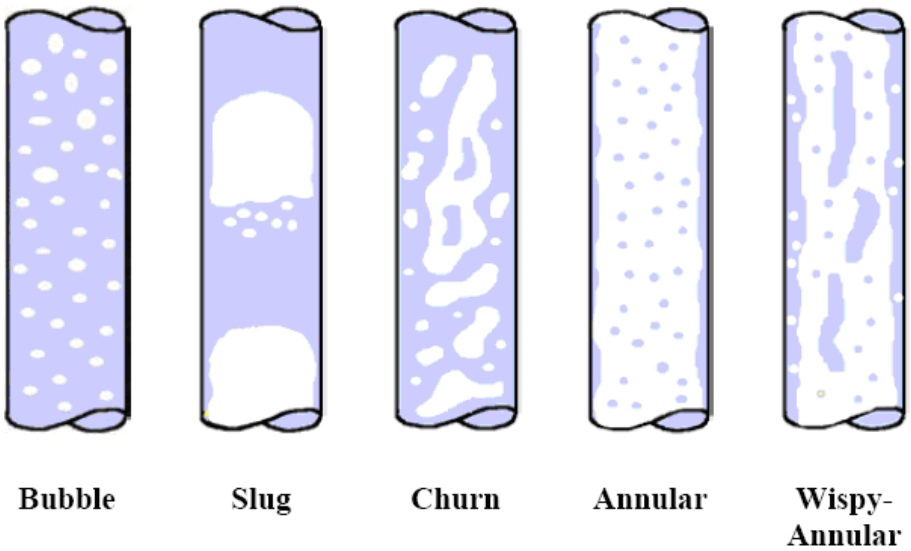

Figure 1.1 Flow patterns in vertical two-phase flow [5]

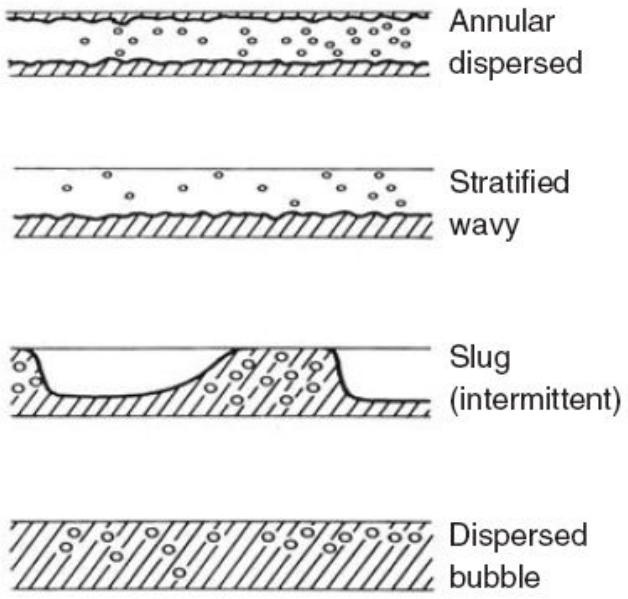

Figure 1.2 Flow patterns in horizontal two-phase flow [14]

The identification and classification of flows into flow patterns, while subjective, has presented a useful approach for the modeling of multiphase flows. In particular, the pressure drop and phase hold-ups differ significantly from one pattern to another and hence the prediction of multiphase flow benefits from knowledge of the flow pattern and subsequently of appropriate relationships specific to the flow pattern in question.

The methods that perhaps offer the best chance of predicting multiphase flows accurately are the phenomenological models. These models rely on the identification of flow patterns and the use of separate bespoke models for each regime. For example, in slug flow the traditional Eulerian solution of a two-fluid model which specifies a stationary spatial grid over which the partial differential equations are discretised, presents certain difficulties associated with the unphysical dispersion of discontinuities, for example, the noses and tails of slugs. These problems can be partly alleviated using complex adaptive grid techniques which allow the spatial nodes to bunch in order to 'resolve' discontinuities. However, perhaps the only robust solution will come from a Langrangian phenomenological model where individual slugs are followed throughout the system and appropriate correlations are employed for entrainment of bubbles at the nose and shedding of liquid from the tail [6].

2.2 Hydrates Formation

The formation of hydrates is a fundamental hindrance in the production of oil and gas through subsea pipelines. The oil, gas and water mixture produced at the wellhead, will normally be at a high pressure and at a moderate temperature. As the mixture flows through the subsea production system and flowlines, it cools down gradually and sometimes rapidly. The mixture will enter the hydrate formation region and the flow path may become restricted or even blocked.

Gas hydrates or clathrate hydrates are ice-like crystalline compounds formed by the inclusion of low molecular diameter organic molecules diameter or organic molecules which is usually gasses, inside cavities formed by water molecules. Clathrates have similar properties to ice but they differ where the formation occurs at temperature above the freezing point of water at elevated pressure conditions. Water molecules through hydrogen bonding can form a lattice-like structure which becomes stable when filled with suitable size gas molecules known as 'hydrate former'. Among the common hydrate formers are natural gas components, methane, ethane, propane, isobutene, nitrogen, hydrogen sulfide and carbon dioxide Gas hydrates can be formed at temperature well above the triple point of water [7].

Gas hydrates found at low temperature and high pressure. When temperature falls, liquids and gas tend to crystallize or freeze. Their molecules vibrates more slowly, and since vibration causes fluids to flow and take the shape of the container rather than act like a solid block of ice or table salt, the removal of thermal energy allows most fluids to freeze into crystalline structure. At higher pressure, warmer fluids can freeze due to the tendency of the pressure to 'push' molecules into the crystalline structure [8].

There are other phenomena that enhance hydrate formation such as turbulence, nucleation sites and free-water. Hydrate formation is favored in regions where the fluid velocity is high. Therefore, choke valves are particularly susceptible to hydrate formation. When natural gas is choked through a valve, there is usually a significant temperature drop because of the Joule-Thomson effect. The velocity is high through the narrowing in the valve. Nucleation site is also favored for hydrate formation since

it is a point at which a phase transition of solid from a fluid phase. These sites include imperfection in the pipeline, a weld spot, a pipeline fitting. The water-gas interface is a good nucleation site for hydrate formation.

To prevent hydrate problems in subsea production systems, several methods can be used. First, the freezing point of the water phase can be lowered by injecting large volumes of chemicals such as methanol. Second, small volumes of additives can be injected to prevent the agglomeration of hydrate crystals. Third, the flowline can be insulated or even heated to maintain the flowing mixture outside the hydrate formation region. In the petroleum industry, methods have been developed to determine the volume of freezing point depressant required, the volume of additive required, and the insulation and degree of heating required [8].

The use of organic hydrates inhibitors such as methanol and ethylene glycol for hydrate prevention is common practice in deepwater operations. However, this poses another problem for flow assurance which is the salt precipitation commonly termed 'salting out' [4].

Petroleum production is commonly associated with the production of saline formation water. NaCl and KCl are the principal electrolyte components of almost all produced water. During production, pressure or temperature changes may result in super-saturation in the produced water and also inducing in salt precipitation (Joseph, James, 2002).

The processes leading to salt precipitation generally follow one of the following scenarios [8].

1. As fluids are transported from the reservoir to the surface, the temperature reduction will result in a reduction in salt solubility.
2. The salt concentration of brines increase as produced gas strips water and leave the salt behind. This phenomenon is assisted by the reduction in the system pressure and therefore resulting in an increase in water partial pressure).
3. Salt solubility in the aqueous phase will reduce with the addition of organic hydrate inhibitor such as methanol and glycol.

4. The deposition of bicarbonates as carbonates with the reduction in CO_2 concentration in the aqueous phase.

Salt precipitation can pose a serious flow assurance problem due to potential salt plug formation in the well-bore, tubing and pipelines. Furthermore, the loss of salt from the aqueous phase may also reduce the hydrate preventive characteristic of the flow system and therefore increase the likelihood of clathrate formation.

The gas gravity method is very simple for predicting the gas hydrate conditions. The gas gravity method was conceived by Katz of the GPSA Data Book. Also, the gas gravity method has served the gas processing industry well, as an initial estimate for a long period of time. Based on GPSA data book, hydrate equation were developed for gasses where specific gravity was known. The available correlations for a specific gravity method to calculate the hydrate formation condition are Sloan, Berge, Motiee and Hammerschmidt correlations [9].

The formation rate of natural gas hydrate is governed by a multitude of factors, including the pressure, temperature and gas composition, also called PVT-effects. Also, the rate of hydrate formation is determined by the combined effects of heat, mass and momentum transport. Cooling is required to remove the hydrate heat of formation. Mass transport is required to dissolve the natural gas in liquid water, and to bring the dissolved gas molecules in contact with a growing hydrate crystal. Momentum transport influences the overall rate of hydrate formation.

2.3 Computational Fluid Dynamics

Finally the advances in Computational Fluid Dynamics (CFD) and their extension to multiphase flow need mention since this perhaps offers a long-term solution to multi dimensional multiphase flows. The fundamental equations of fluid mechanics can be averaged and discretised in three dimensions for multiphase flows and have produced successful solutions to engineering problems. However, as with all of the methods described, the ultimate accuracy depends intrinsically on the empirical relationships that are provided to close the model, and this is where these advance methods need additional improvement. Furthermore, for the specific

problem of multiphase flows in risers which have large L/D ratios, it is difficult to see how the application of CFD could yield practical engineering solutions without very substantial improvement in computing power.

Rigorous two phase modeling has been one of the great challenges in the classical science. As with most problems in engineering, the interest in two-phase flow is due to its extremely importance in various industry application. Two-phase computational fluid dynamics (CFD) calculations, using Eulerian model and commercial CFD packages FLUENT 6.2, is suitable to calculate the gas-liquid flow in pipe.

Given gas and liquid flow rates, the global determination of both pressure drop and phase distribution (gas holdup) will strongly depend on the momentum transfer modeling. In a global approach of the problem, it is then necessary to propose three closure relations to express momentum transfer coefficients. One of the early CFD models is the turbulent stratified flow in a horizontal pipe [10]. Numerically simulated stratified gas-liquid pipe flow was done using standard k-ε turbulence model with the wall functions for each phase [11]. More satisfactory solutions for stratified pipe flow by employing a low Reynolds number turbulent model instead of wall functions [12].

Continuity Equation [16]

$$\frac{\partial \overline{U}}{\partial X} + \frac{\partial \overline{V}}{\partial Y} + \frac{\partial \overline{W}}{\partial Z} = 0 \tag{2.31}$$

Momentum Equation

$$\frac{D\overline{U}_j}{Dt} = -\frac{\partial(\overline{P} + 2k_n/3)}{\partial X_j} + \frac{1}{\mathrm{Re}}\frac{\partial}{\partial X_i}\left[\left(1+\upsilon_{t,n}\right)\cdot\left(\frac{\partial \overline{U}_i}{\partial X_j} + \frac{\partial \overline{U}_j}{\partial X_i}\right)\right] \tag{2.32}$$

K-Equation

$$\frac{Dk_n}{Dt} = \frac{1}{\mathrm{Re}}\frac{\partial}{\partial X}\left[\frac{\upsilon_{t,n}}{\sigma_k}\frac{\partial k_n}{\partial X}\right] + \frac{1}{\mathrm{Re}}\frac{\partial}{\partial Y}\left[\frac{\upsilon_{t,n}}{\sigma_k}\frac{\partial k_n}{\partial Y}\right] + \frac{1}{\mathrm{Re}}\frac{\partial}{\partial Z}\left[\frac{\upsilon_{t,n}}{\sigma_k}\frac{\partial k_n}{\partial Z}\right] + G_n - \varepsilon_n \tag{2.33}$$

ε -Equation

$$\frac{D\varepsilon_n}{Dt} = \frac{1}{\mathrm{Re}}\frac{\partial}{\partial X}\left[\frac{\upsilon_{t,n}}{\sigma_k}\frac{\partial \varepsilon_n}{\partial X}\right] + \frac{1}{\mathrm{Re}}\frac{\partial}{\partial Y}\left[\frac{\upsilon_{t,n}}{\sigma_k}\frac{\partial \varepsilon_n}{\partial Y}\right] + \frac{1}{\mathrm{Re}}\frac{\partial}{\partial Z}\left[\frac{\upsilon_{t,n}}{\sigma_k}\frac{\partial \varepsilon_n}{\partial Z}\right] + C_{1\varepsilon}\frac{\varepsilon_n}{k_n}G_n + C_{2\varepsilon}\frac{\varepsilon^2}{k_n} \tag{2.34}$$

The previous equations can be solved in the domain interest in order to simulate a turbulent flow situation. If a grid situation is set for a given flow domain, then the boundary conditions can be worked out.

The Standard $K-\varepsilon$ Model [16].

The turbulent viscosity model is as the following equation:

$$\overline{-u_i'u_j'} = \upsilon_t\left(\frac{\partial \overline{u}_i}{\partial \overline{x}_j} + \frac{\partial \overline{u}_j}{\partial \overline{x}_i}\right) - \frac{2}{3}k\delta_{ij} \tag{2.35}$$

υ_t is the turbulent eddy viscosity, δ_{ij} is the Kronecker delta . The turbulent eddy viscosity is calculated from the velocity scale $k^{\frac{1}{2}}$ and the length scale of $\frac{k^{\frac{2}{3}}}{\varepsilon}$ which were developed empirically. The term ε is the dissipation rate while the term k is the kinetic energy.

$$\frac{\partial k}{\partial t} + \overline{u}_i\frac{\partial k}{\partial x_i} = \frac{\partial}{\partial x_i}\left(\frac{\upsilon_t}{\sigma_k}\frac{\partial k}{\partial x_i}\right) + \upsilon_t\left(\frac{\partial \overline{u}_i}{\partial x_j} + \frac{\partial \overline{u}_j}{\partial x_i}\right)\frac{\partial \overline{u}_i}{\partial x_j} - \varepsilon \tag{2.36}$$

$$\frac{\partial \varepsilon}{\partial t} + \overline{u}_i\frac{\partial \varepsilon}{\partial x_i} = \frac{\partial}{\partial x_i}\left(\frac{\upsilon_t}{\sigma_\varepsilon}\frac{\partial \varepsilon}{\partial x_i}\right) + C_{1\varepsilon}\frac{\varepsilon}{k}G - C_{2\varepsilon}\frac{\varepsilon^2}{k} \tag{2.37}$$

$$G = \upsilon_t\left(\frac{\partial \overline{u}_i}{\partial x_j} + \frac{\partial \overline{u}_j}{\partial x_i}\right)\frac{\partial \overline{u}_i}{\partial x_j} \tag{2.38}$$

where G is the generation of k. The turbulent viscosity is then related to k and ε by the following expression:

$$\upsilon_t = C_\mu\frac{k^2}{\varepsilon} \tag{2.39}$$

The coefficients $C_\mu = 0.09,\ C_{1\varepsilon} = 1.44,\ C_{2\varepsilon} = 1.92,\ \sigma_k = 1.0, \sigma_\varepsilon = 1.3$. These values have been empirically determined. The equation for the turbulent kinetic energy determines the velocity scale [13].

The thermal energy or the concentration conservation equation or also known as the energy equation is not used during this analysis because the analysis does not involve heat transfer. The following conservation equations are utilized in the $K-\varepsilon$ Model. The barred values are considered as the time –averaged values,

The pressure gradient in the two phase flow can be express as the sum of three components due to friction, gravity and acceleration [14],

$$-\frac{dp}{dx} = \tau_{wg}\frac{P_g}{A} + \tau_{wl}\frac{P_l}{A} + \left(\alpha_g\rho_g + \alpha_l\rho_l\right)gsin\theta + \frac{d}{dx}\left[\rho_g\frac{u_{sg}^2}{\alpha_g} + \rho_l\frac{u_{sl}^2}{\alpha_l}\right] \quad (2.40)$$

2.3.1 Boundary Conditions and Interface Treatment

2.3.1.1 Boundary conditions at inlet

At the inlet, uniform profiles for all the dependent variables were employed [13]:

$$u_n = U_0$$

where u_n is normal velocity perpendicular to the inlet plane. The gravitation direction is downward or in the opposite direction of the inlet velocity.

2.3.1.2 Boundary conditions at wall

A non-slip boundary condition is imposed on the wall of the pipe. The two-layer based non-equilibrium wall function method was used to account for the near wall regions in the numerical computation of turbulent flow. In the near wall cell, the value of the dissipation rate of the turbulent kinetic energy is given by [13]

$$\varepsilon = \frac{C_\mu^{3/4}k^{3/2}}{ky}$$

2.3.1.3 Boundary condition at the outlet

The outlet boundary condition is recommended to be set up as a pressure outlet boundary instead of as an outflow boundary to avoid difficulties with backflow. The diffusion flux for the entire variables in exit direction was set to be zero [13].

$$\frac{\partial}{\partial n}(u, k, \varepsilon) = 0$$

2.4 Empirical Correlations for Natural Gas Hydrates Predictions

The available equations for predicting hydrates temperature are [9]:

2.4.1 Berge method

For $0.555 \leq \gamma_g < 0.58$ [9]

$T = -96.03 + 25.37 \times \ln P - 0.64 \times (\ln P)^2 + (\gamma_g - 0.555)/0.025 \times [80.61 \times P + 1.16\times10^4 / (P + 596.16) - (-96.03 + 25.37 \times \ln P - 0.64 \times (\ln P)^2)]$

And for $0.58 \leq \gamma_g < 1.0$

$T = \{80.61 \times P - 2.1\times10^4 - 1.22\times10^3/ (\gamma_g - 0.535) - [1.23\times10^4 + 1.71\times10^3/ (\gamma_g - 0.509)]\}/[P - (-260.42-15.18/(\gamma_g-0.535))]$

Both the above equation are temperature explicit where temperature is calculated directly for a given pressure and specific gravity of the gas.

2.4.2 Hammerschmidt method

Hammerschmidt gives the following relationship for initial hydrate forming temperature below [9]:

$$T = 8.9\ P^{0.285}$$

By transforming to pressure explicit form, the equation for initial pressure calculation becomes;

$$P = (T/8.9)^{3.509}$$

2.4.3 Motiee method

A regression method was use to determine six coefficients that would correlate temperature, pressure and specific gravity. The equations are as follows [9]:

$$\text{Log (P)} = a_1 + a_2T + a_3T^2 + a_4\gamma_g + a_5\gamma_g{}^2 + a_6T\gamma_g$$

$$T = b_1 + b_2\text{Log (P)} + b_3 (\text{Log(P)})2 + b_4\gamma_g + b_5\gamma_g{}^2 + b_6\gamma_g \text{ Log (P)}$$

2.4.4 Sloan method

A regression method was used to determine fifteen coefficients that would correlate temperature, pressure and specific gravity. The correlation was fit in the temperature range 34 to 60^{o}F, the pressure range of 65 to 1500 psi, and the gas gravity range from 0.552 to 0.9. The equations are as follows [9]:

$$T = 1/[\, c1 + c2 (\ln p) + c3 (\ln \gamma) + c4 (\ln p)^2 + c5 (\ln p)(\ln \gamma) + c6 (\ln \gamma)^2 + c7 (\ln p)^3 + c8 (\ln \gamma)(\ln p)^2 + c9 (\ln \gamma)^2(\ln p) + c10(\ln \gamma)^3 + c11(\ln \gamma)^4 + c12(\ln \gamma)(\ln p)^3 + c13(\ln \gamma)^2(\ln p)^2 + c14(\ln \gamma)^3 (\ln p) + c15 (\ln \gamma)^4]$$

The coefficients for this correlation are:

Table 2.1 Coefficients for Calculating the Hydrate-Formation Temperature [15]

$C_1 = 2.7707715 \times 10^{-3}$	$C_2 = -2.782238 \times 10^{-3}$	$C_3 = -5.649288 \times 10^{-4}$
$C_4 = -1.298593 \times 10^{-3}$	$C_5 = 1.407119 \times 10^{-3}$	$C_6 = 1.785744 \times 10^{-4}$
$C_7 = 1.130284 \times 10^{-3}$	$C_8 = 5.9728235 \times 10^{-4}$	$C_9 = -2.3279181 \times 10^{-4}$
$C_{10} = -2.6840758 \times 10^{-3}$	$C_{11} = 4.6610555 \times 10^{-3}$	$C_{12} = 5.5542412 \times 10^{-4}$
$C_{13} = -1.4727765 \times 10^{-5}$	$C_{14} = 1.3938082 \times 10^{-5}$	$C_{15} = 1.4885010 \times 10^{-6}$

CHAPTER 3
METHODOLOGY OF PROJECT WORK

3.1 Introduction

This section provides with the data and procedures which are use in this project. There are two distinct phases which will be described in details in this chapter.

The first phase is through understanding of the multiphase flow to gain big picture of the flow assurance in riser pipeline. One of the most important elements is to get information on the principals and theory of flow inside riser. Next, it is important to acquire data of fluid flow parameters for modeling. This is done through data gathering of fluid properties and empirical methods. The hydrocarbon properties are such as compositions, density, viscosity, pressure, and temperature. Besides that, the properties of a riser are needed such as diameter, length, grade, nominal size and surface roughness.

The second phase will be using the Computational Fluid Dynamics (CFD) methods. The CFD software used for the simulation of the multi-phase flow in the riser is FLUENT 6.2 together with the GAMBIT preprocessor.

3.2 Flow Parameters

As in any modeling, some sort of dynamic similarity is required between the model and the actual system undergoing the phenomenon researched. Some of the parameter input used in this particular simulation is determined by empirical methods.

3.2.1 Volume Fraction and Density

The volume fraction of the dispersed phase is defined as

$$\alpha_d = \lim_{\delta V \to V^o} \frac{\delta V_d}{\delta V}$$

where δV_d is the volume of the dispersed phase in volume δV. The volume δV^o is the limiting volume that ensures a stationary average. Unlike a continuum, the volume fraction cannot be defined at a point. Equivalently, the volume fraction of the continuous phase is

$$\alpha_c = \lim_{\delta V \to V^o} \frac{\delta V_c}{\delta V}$$

where δV_c is the volume of the continuous phase in the volume. This volume fraction is sometimes referred to as the void fraction and in the chemical engineering literature, the volume fraction of the dispersed phase is often referred to as holdup. By definition, the sum of the volume fractions must be unity,

$$\alpha_d + \alpha_c = 1$$

The bulk density (or apparent density) of the dispersed phase is the mass of the dispersed phase per unit volume of mixture or, in terms of a limit, is defined as

$$\bar{\rho}_d = \lim_{\delta V \to V^o} \frac{\delta M_d}{\delta V}$$

where δM_d is the mass of the dispersed phase. The bulk density is related to the material density ρ_d by

$$\bar{\rho}_d = \alpha_d \rho_d$$

The sum of the bulk densities for the dispersed and continuous phases is the mixture density

$$\bar{\rho}_d + \bar{\rho}_c = \rho_m$$

3.2.2 Superficial and Phase Velocity

For multiphase flow in a pipe, the superficial velocity of each phase is the mass flow rate $\dot{M}$ of that phase divided by the pipe A and material density which is defined as

$$U_d = \frac{\dot{M}_d}{\rho_d A}$$

The superficial velocity U_d and phase velocity, u_d are related by the volume fraction

$$U_d = \alpha_d u_d$$

3.2.3 Fluid Properties

In this modeling of multiphase flow, a two phase flow is taken as a subject of study. Therefore, the properties of each phase are determined where in a pipeline consists of gas-liquid flow. The component for gas phase is methane while the component for liquid phase is water-liquid.

Table 3.1 Fluid Properties

Operating Pressure	9590000 Pa
Operating Temperature	288.16 K
Gas volume fraction	0.85
Liquid volume fraction	0.15
Gas velocity	12.5 m/s
Liquid velocity	0.1 m/s
Mixture velocity inlet	10.64 m/s

3.2.4 Pipeline Properties

Table 3.2 Pipeline Properties

Pipe diameter	0.2 meter
Pipe length	50 meter
Material	Steel
Wall thickness	0.02 meter
Roughness height	0.00002
Roughness constant	0.5

3.3 CFD modeling

This work will be presented in the chronological order in which it was carried out. The first step in the analysis is preprocessing which involves building a geometrical model in GAMBIT, applying a finite-volume based mesh, and entering data. Once the numerical model is prepared, it is exported to FLUENT 6.2 to perform the necessary calculations and produced the desired results.

3.3.1 Gambit Software

Gambit is Fluent's geometry and mesh generation software. Gambit's single interface for geometry creation and meshing brings together most of Fluent's preprocessing technology in one environment. A 3-Dimensional geometrical model of a pipeline segment was created according to the specification decided earlier (refer section 3.2). The model was then meshed according to the following specifications:

- Meshing elements: Hex/Wedge
- Mesh type: Cooper
- Mesh size: 0.01 (interval size)
- Boundary condition at inlet: velocity inflow
- Boundary condition at outlet: pressure outflow

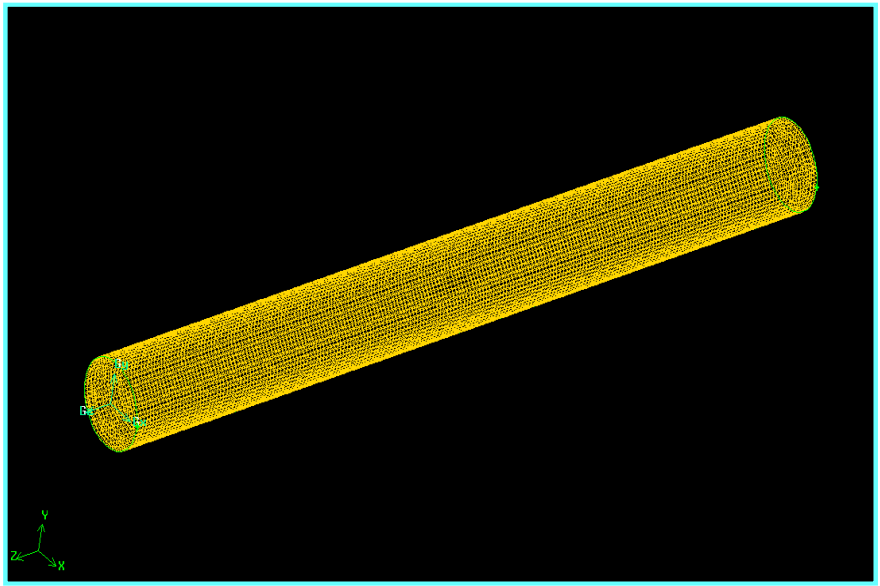

Figure 3.1 Geometry model of pipeline segment in Gambit

3.3.2 Fluent Software

The commercial CFD software package, FLUENT 6.2, which is based on the finite volume approach, was used for solving the set of governing equations. The meshed model from Gambit was imported into FLUENT 6.2, and the simulation of the two-phase flow was performed according to the following procedure:

3.3.2.1 3D, segregated, VOF, Standard k-epsilon

Table 3.3 Model Settings for Fluent Software

Model	Settings
Space	3D
Time	Steady
Viscous	Standard k-epsilon turbulence model
Wall Treatment	Standard Wall Functions
Heat Transfer	Enabled
Solidification and Melting	Disabled
Radiation	None
Species Transport	Disabled
Coupled Dispersed Phase	Disabled
Pollutants	Disabled
Soot	Disabled

3.3.2.2 Boundary Conditions

Table 3.4 Boundary Conditions for Zone Types

Name	Id	Type
Volume1	2	Fluid
Outflow2	4	Outflow
Inflow1	5	Velocity-inlet
Wall	3	Wall
Default-interior	7	Interior

Tables 3.5 Boundary Conditions for Outfow2

Condition	Value
Flow rate weighting	1

Table 3.6 Boundary Conditions for Inflow1

Condition	Value
Velocity Specification Method	2
Reference Frame	0
Velocity Magnitude	10.64
Temperature	290
Turbulence Specification Method	3
Turbulence Kinetic Energy	1
Turbulence Dissipation Rate	1
Turbulence Intensity	0.079999998
Turbulence Length Scale	1
Hydraulic Diameter	0.2
Turbulent Viscosity Ratio	10

Table 3.7 Boundary Conditions for Wall

Condition	Value
Wall Thickness	0.02
Material Name	Steel
Temperature	282
Enable shell conduction?	no
Wall Motion	0
Shear Boundary Condition	0
Define wall motion relative to adjacent cell zone?	Yes
Apply a rotational velocity to this wall?	No
Wall Roughness Height	1.9999999e-05
Wall Roughness Constant	0.5

3.3.2.3 Solver Control

Table 3.8 Solver Control for Equations

Equation	Solved
Flow	Yes
Volume Fraction	Yes
Turbulence	Yes
Energy	Yes

Table 3.9 Solver Control for Numeric

Numeric	Enabled
Absolute Velocity Formulation	Yes

Table 3.10 Solver Control for Relaxation

Variable	Relaxation Factor
Pressure	0.30000001
Density	1
Body Forces	1
Momentum	0.69999999
Volume Fraction	1
Turbulence Kinetic Energy	0.80000001
Turbulence Dissipation Rate	0.80000001
Turbulent Viscosity	1
Energy	1

Table 3.11 Linear Solver

Variable	Solver Type	Termination Criterion	Residual Reduction Tolerance
Pressure	V-Cycle	0.1	
X-Momentum	Flexible	0.1	0.7
Y-Momentum	Flexible	0.1	0.7
Z-Momentum	Flexible	0.1	0.7
Volume Fraction	Flexible	0.1	0.7
Turb. Kinetic Energy	Flexible	0.1	0.7

Table 3.11 Linear Solver (continue)

Turb. Dissipation Rate	Flexible	0.1	0.7
Energy	Flexible	0.1	0.7

Table 3.12 Discretization Scheme

Variable	Scheme
Pressure	Standard
Momentum	First Order Upwind
Volume Fraction	First Order Upwind
Turbulence Kinetic Energy	First Order Upwind
Turbulence Dissipation Rate	First Order Upwind
Energy	First Order Upwind

Table 3.13 Solution Limits

Quantity	Limit
Minimum Absolute Pressure	1
Maximum Absolute Pressure	5e+10
Minimum Temperature	1
Maximum Temperature	5000
Minimum Turb. Kinetic Energy	1e-14
Minimum Turb. Dissipation Rate	1e-20
Maximum Turb. Viscosity Ratio	100000

3.3.2.4 Material Properties

Table 3.14 Material Properties for steel (solid)

Property	Units	Method	Value(s)
Density	kg/m3	Constant	8030
Cp (Specific Heat)	j/kg-k	Constant	502.48
Thermal Conductivity	w/m-k	Constant	16.27

Table 3.15 Material properties for water-liquid (fluid)

Property	Units	Method	Value(s)
Density	kg/m3	Constant	998.2
Cp (Specific Heat)	j/kg-k	Constant	4182
Thermal Conductivity	w/m-k	Constant	0.6
Viscosity	kg/m-s	Constant	0.001003
Molecular Weight	kg/kgmol	Constant	18.0152
Standard State Enthalpy	j/kgmol	Constant	0
Reference Temperature	k	Constant	298.15

Table 3.16 Material properties for methane (fluid)

Property	Units	Method	Value(s)
Density	kg/m3	Constant	0.6679
Cp (Specific Heat)	j/kg-k	Constant	2222
Thermal Conductivity	w/m-k	Constant	0.0332
Viscosity	kg/m-s	Constant	1.087e-05
Molecular Weight	kg/kgmol	Constant	16.04303
Standard State Enthalpy	j/kgmol	Constant	-74895176
Reference Temperature	k	Constant	298.15

3.4 Flow Chart of Project Executive

Below are the steps or procedures taken to complete the whole project:

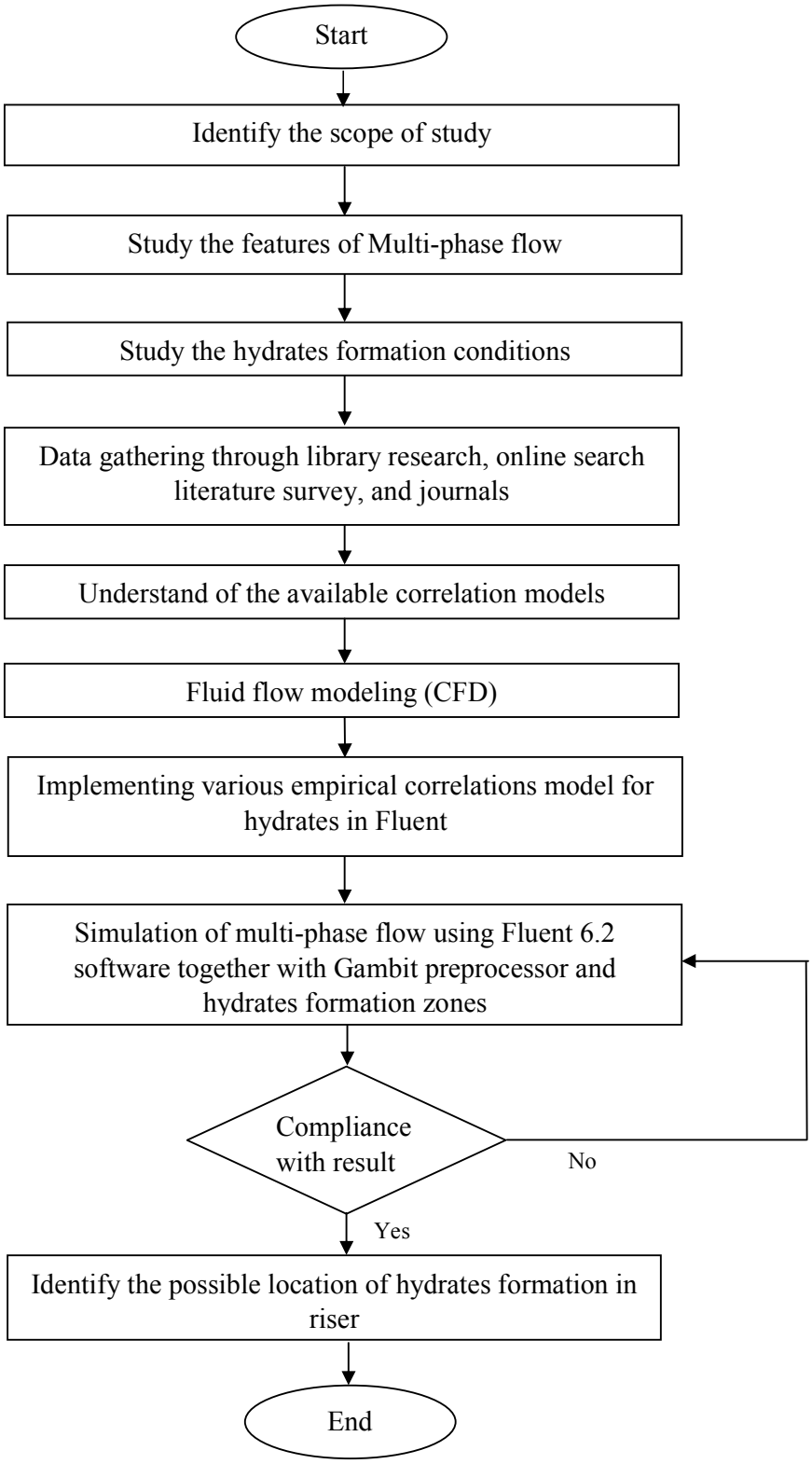

Figure 3.2 Flow Chart indicating the steps taken during the entire project

3.5 Tools

As mentioned above, there are three main software applications involved in this final year project which are:

- FLUENT 6.2
- GAMBIT 2.2
- Microsoft Office

There are few reasons to choose FLUENT 6.2 as the CFD simulation in this project. FLUENT offers;

- A wide range of proven and leading edge Multiphase models which will sure help in CFD simulation of multiphase flow in riser of deep oil well.
- Advanced meshing tools
- Optimal Parallelization schemes
- World wide experience and involvement in Multiphase applications

GAMBIT will be used to model the segment of the riser flow system before further processing with FLUENT software as solver. GAMBIT is chosen over FLUENT to carry out the preprocessing stage for geometry modeling and mesh generation. The selection of this software is that software license is available in the computer lab of Mechanical department. All the simulation work was done on a Pentium IV-based computer with 2 GB RAM, 40 GB hard disk and an operational speed of 2.7 GHz.

Microsoft Office is chosen because it is a powerful office application suite which will be an essential tool in preparing the reports and spreadsheet calculations throughout the project.

CHAPTER 4
RESULTS AND DISCUSSION

4.1 Introduction

This chapter presents the results of the simulations of the two-phase flow in a pipe. The two-phases are the methane gas and water-liquid. The results are displayed in several ways which are shown by colour-filled contour maps depicting the distribution of turbulence, pressure, temperature and volume fraction. The discussion follows closely will explain further.

Since the simulations is best done in 3-dimensional to monitor the flow and its characteristics throughout the pipe in all direction, it is better to display the results of the simulation in 2-dimensional for better analysis. This can be done through the cross sectional view of the pipe along the longitudinal axis. From the results of these cross sectional view, the pressure drop, temperature drop distribution can be notices as the two-phase flow travel along the pipe. Other than that, the distribution of each phase of methane and liquid-water can be view best in 2-dimensional pipe. In addition, the data of the results gathered from the simulation are to be used in the calculation of the hydrates conditions with the use of empirical correlations. These results are compared in graphical method for further analysis of the hydrates condition.

It has to be noted that in this CFD modelling of multiphase flow, a segment of the pipe was taken for analysis. Therefore, a certain amount of pipe length is taken as the geometry of the pipe to perform simulation in FLUENT 6.2. It will be interesting to see the results with respect to the two-phase flow that is subject to analysis in a pipe.

4.2 Simulation Results and Discussion

The simulation of two-phase flow in a 2 meter pipe is shown as below

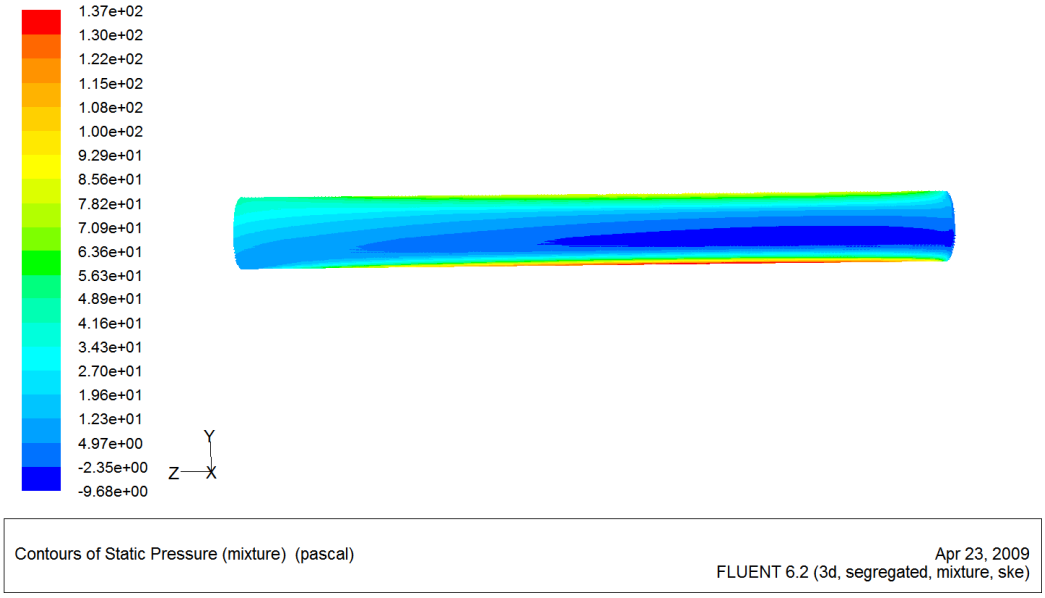

Figure 4.1 Contours of Static Pressure for 2m pipeline

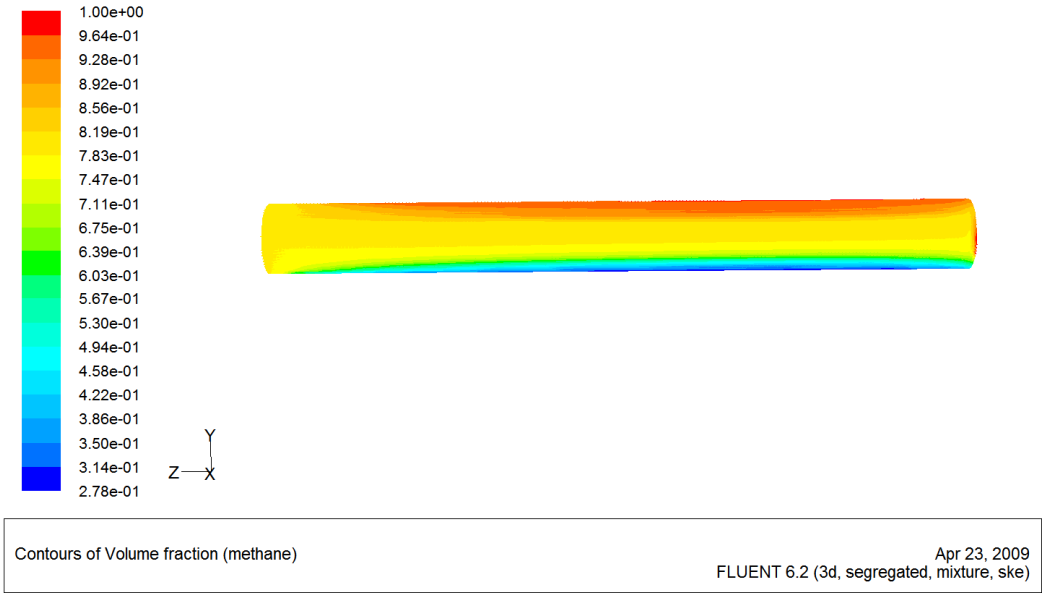

Figure 4.2 Contours of Volume Fraction (methane) for 2m pipeline

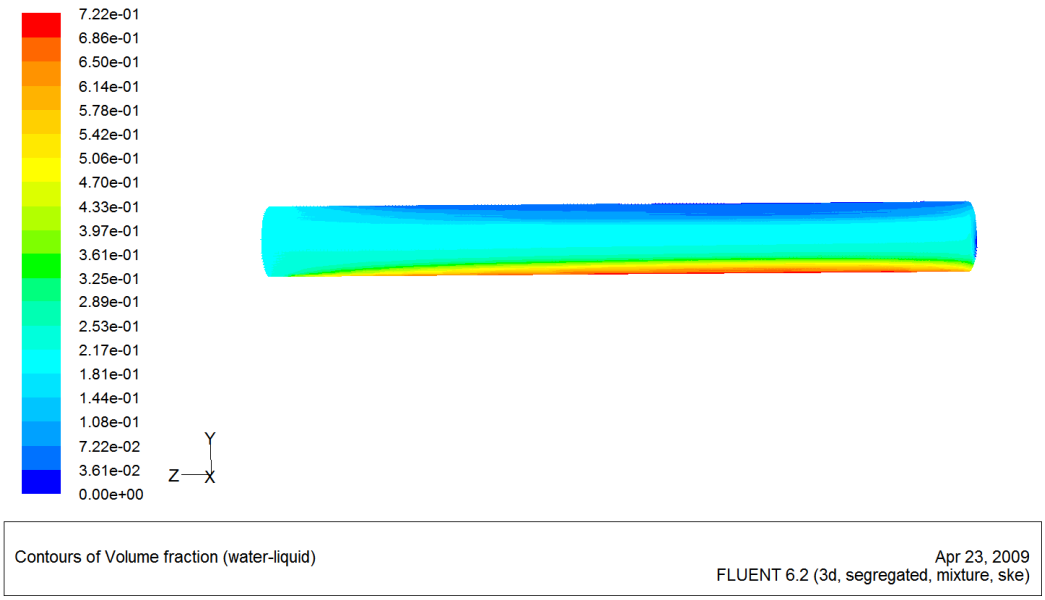

Figure 4.3 Contours of Volume Fraction (water-liquid) for 2m pipeline

From the results of the simulation of the 2-phase flow contains methane gas and water-liquid along a shorter pipe length of 2 meter, it is obvious that the temperature drop will be insignificant as the temperature maintain a constant value. The drop in temperature can only be noticed when the fluid flow through at least a certain of minimum pipe length. However, the segregation of flow and its properties such as pressure and it phases can be noticed from the simulation of shorter pipe length.

Therefore, figure 4.1 shows the contours of static pressure along the 2m pipe which is to the right (negative z direction). There is slightly a small pressure drop as the 2-phases flows along the pipe. The much higher pressure at the bottom of the pipe is due the accumulation of small amount of water-liquid. The lower pressure is notice at the top of the pipe where mostly the methane gas occupied.

Figure 4.2 and 4.3 further illustrate the explanation above. The volume fraction of methane is high at the top of the pipe while the volume fraction of water-liquid is high at the bottom of the pipe. This is due to the density of the gas is much lighter that liquid water.

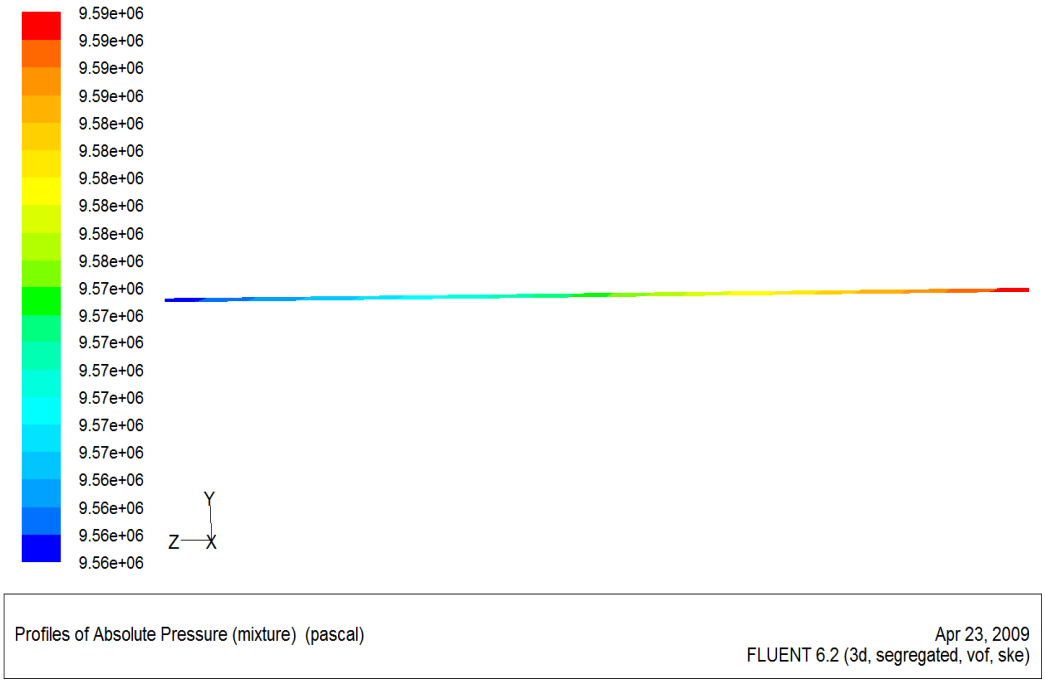

Figure 4.4 Contours of Absolute Pressure along 50m pipeline

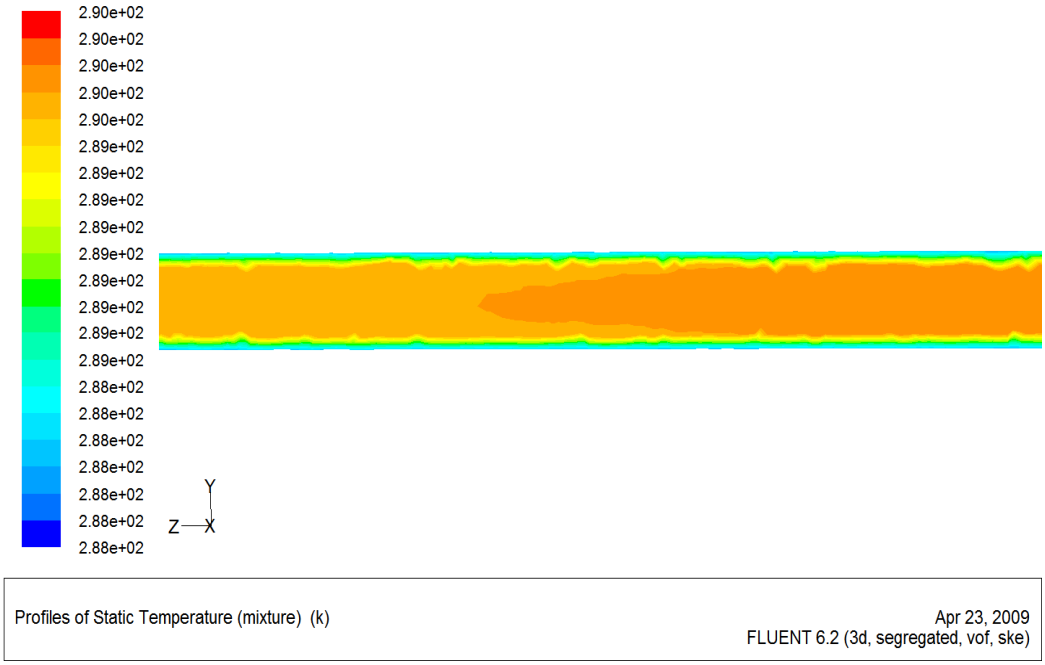

Figure 4.5 Contours of Static Temperature at zoomed position of 22-28m along 50m pipeline

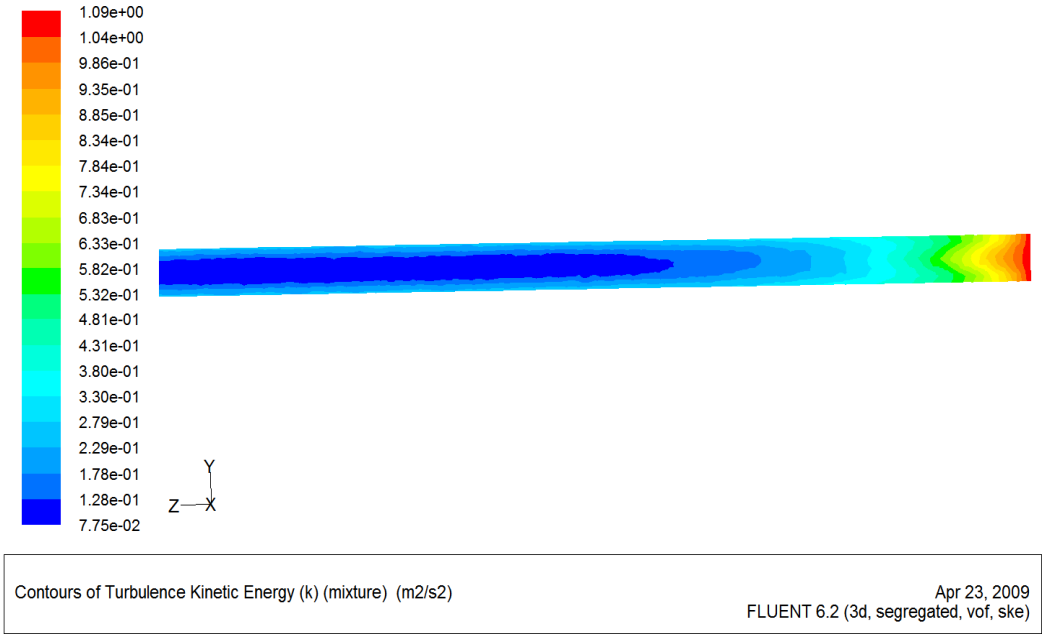

Figure 4.6 Contours of Turbulence Kinetic Energy at zoomed position of 0-10m along 50m pipeline

Figure 4.4 shows the contours of absolute pressure along the 50m pipeline. As the 2-phase flow through the pipe, there is a pressure drop. As stated early, the key aspect of gas-liquid flow in pipeline is also depends on the pressure gradient. This is expected as shown by the change in colour contours along the pipeline.

Figure 4.5 shows the contours of static temperature along the 50m pipeline. Due to the ambient temperature which is lower than the 2-phase flow inside the pipeline, a temperature drop is expected. The pipeline wall shows lower temperature as it is in contact with the sea water (ambient temperature). Loss in the heat energy from the 2-phase flow through the pipeline wall to the surrounding will cause further temperature drop.

Figure 4.6 shows the contour of turbulence kinetic energy of the flow. The characteristic features of 2-phase flow in the pipeline is that the liquid holdup being different from the liquid volume fraction due to slip between the phases. The slip effect is different for different flow patterns. In the horizontal flow, gravity tends to have effect on the phase distribution. Due to high gas-liquid ratio, it is predicted that annular flow exist where liquid film is thin at the top of the pipe and thin at the top of the pipe.

The data extracted from the simulation results is simplified to suitable units for the application of empirical correlation method calculations and the plotting of graph using Microsoft Excel.

Table 4.1 Pressure and Temperature variation along 50m pipeline extracted from simulation

Length	Pressure		Temperature	
(m)	Pa	PSI	kelvin	^{o}C
0	9590010	1390.92	290	17
5	9586930	1390.47	289.927	16.927
10	9583970	1390.04	289.849	16.849
15	9580790	1389.58	289.771	16.771
20	9577720	1389.14	289.694	16.694
25	9574160	1388.62	289.617	16.617
30	9570720	1388.12	289.541	16.541
35	9567670	1387.68	289.466	16.466
40	9564620	1387.24	289.392	16.392
45	9562090	1386.87	289.319	16.319
50	9558980	1386.42	289.245	16.245

Table 4.2 Mathematical model of hydrate formation temperatures for different empirical method

Length	Hammerschmidt		Sloan		Berge	
(m)	^{o}F	^{o}C	^{o}F	^{o}C	^{o}F	^{o}C
0	70.021	21.102	74.572	23.627	54.065	12.246
5	70.015	21.098	74.586	23.635	54.060	12.243
10	70.009	21.095	74.600	23.643	54.055	12.240
15	70.002	21.091	74.615	23.651	54.049	12.237
20	69.996	21.088	74.629	23.659	54.044	12.235
25	69.988	21.084	74.646	23.669	54.038	12.231
30	69.981	21.080	74.662	23.678	54.032	12.228
35	69.975	21.076	74.677	23.686	54.027	12.225
40	69.969	21.073	74.691	23.694	54.022	12.222
45	69.963	21.070	74.703	23.700	54.018	12.220
50	69.957	21.066	74.718	23.708	54.013	12.217

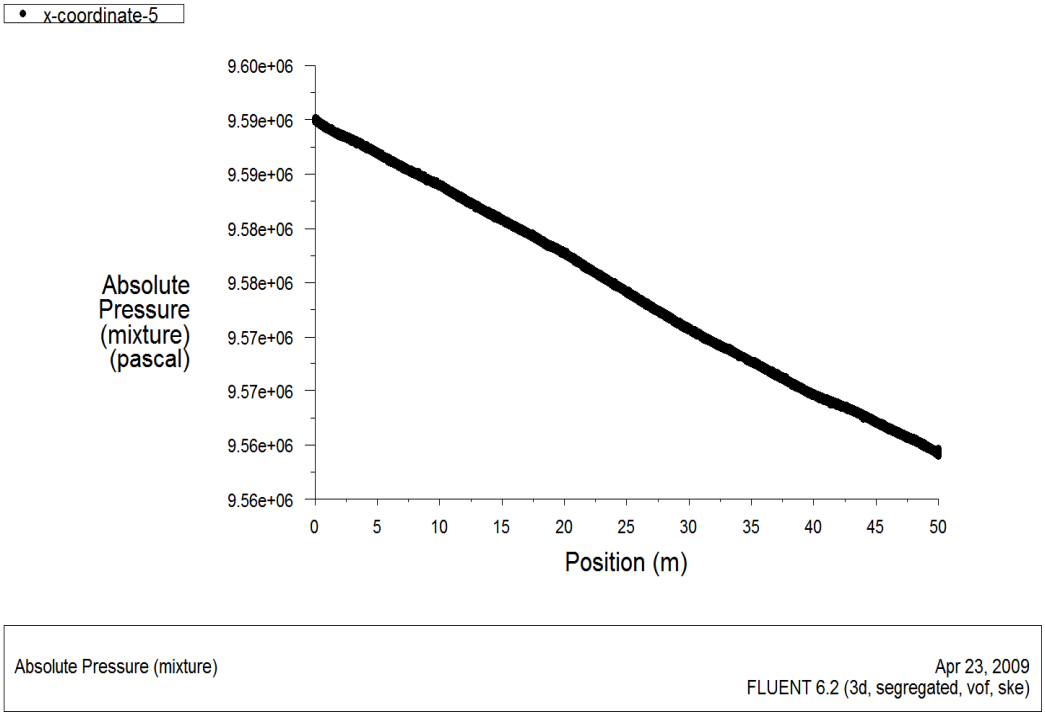

Figure 4.7 Pressure drop along 50m pipeline

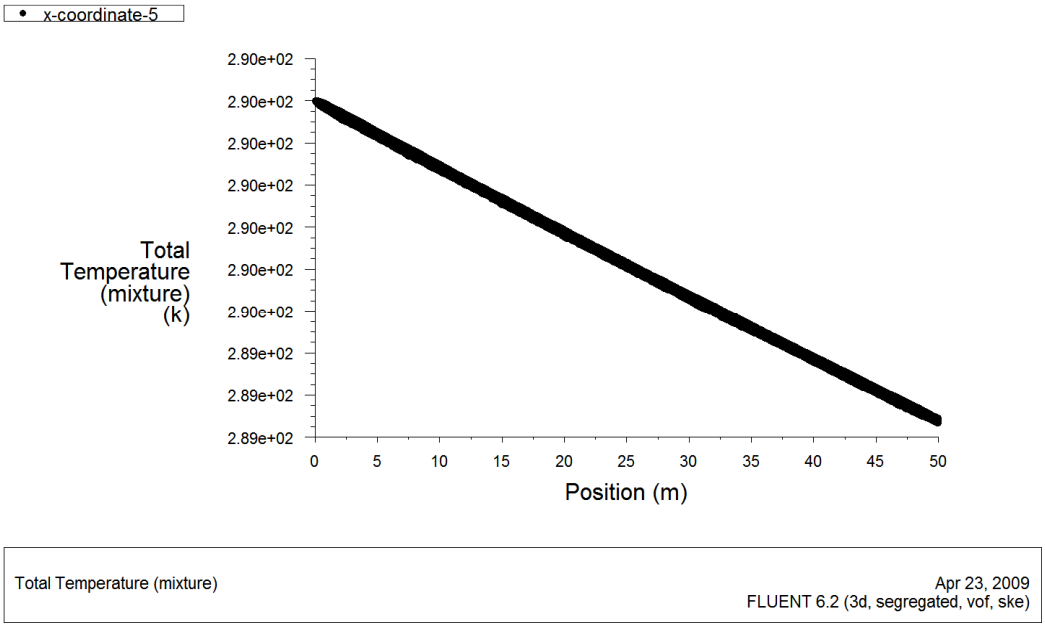

Figure 4.8 Total Temperature along 50m pipeline

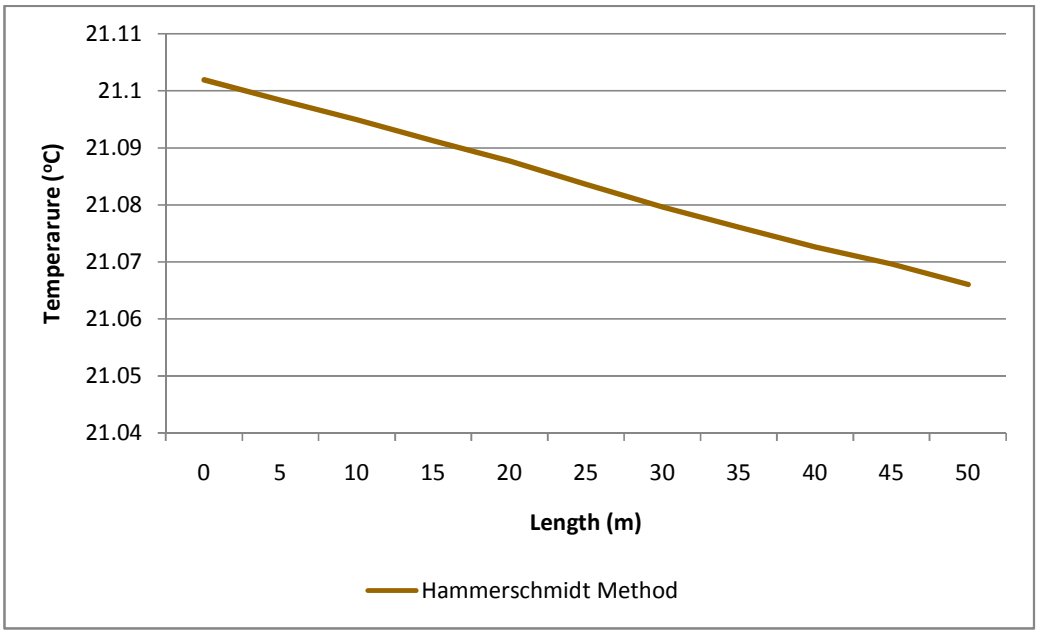

Figure 4.9 Hydrate formation temperatures calculated using Hammerschmidt method versus length of the pipeline.

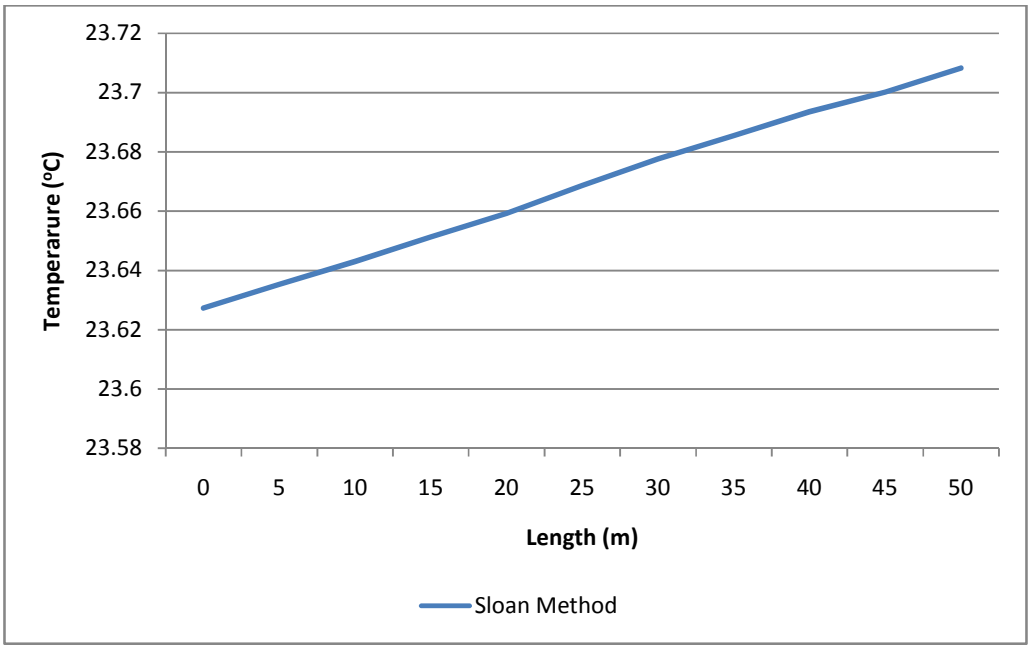

Figure 4.10 Hydrate formation temperatures calculated using Sloan method versus length of the pipeline

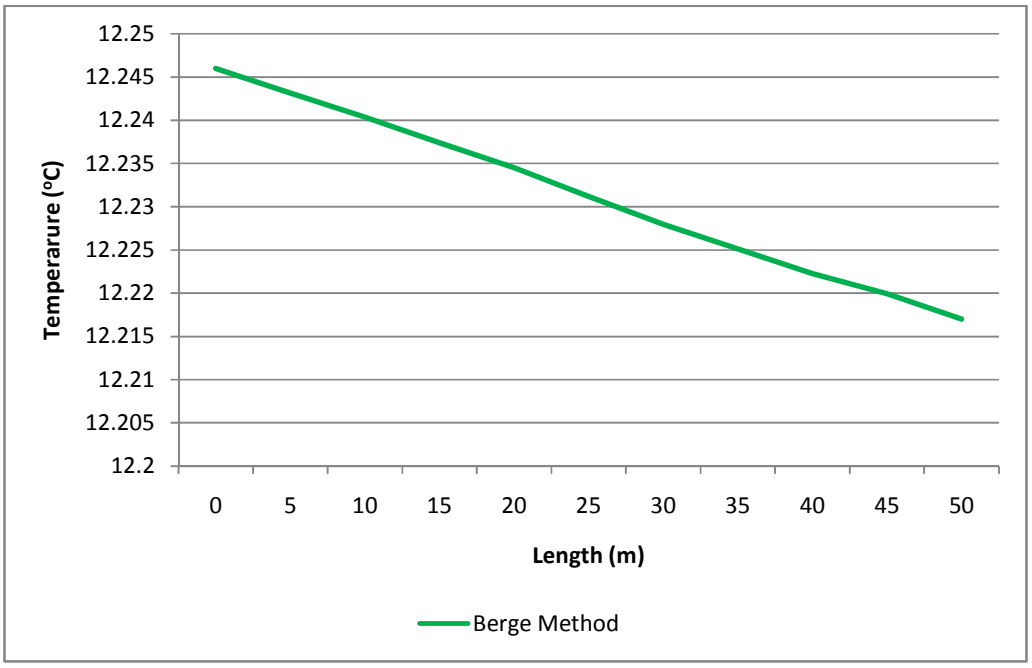

Figure 4.11 Hydrate formation temperatures calculated using Berge method versus length of the pipeline

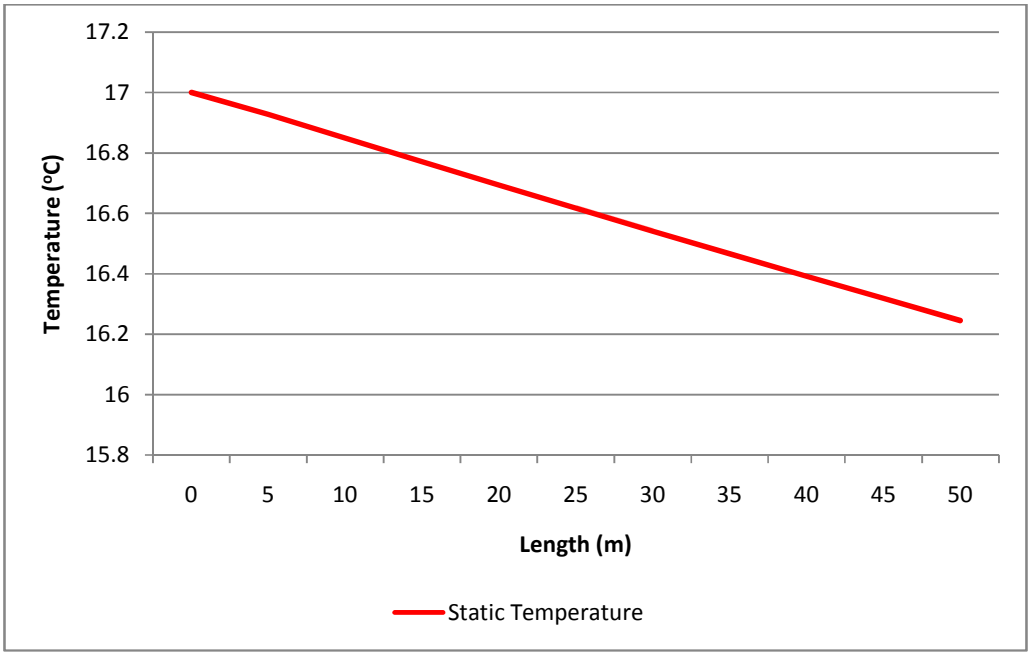

Figure 4.12 Static temperature of the 2-phase flow along 50 meter pipeline from simulation results

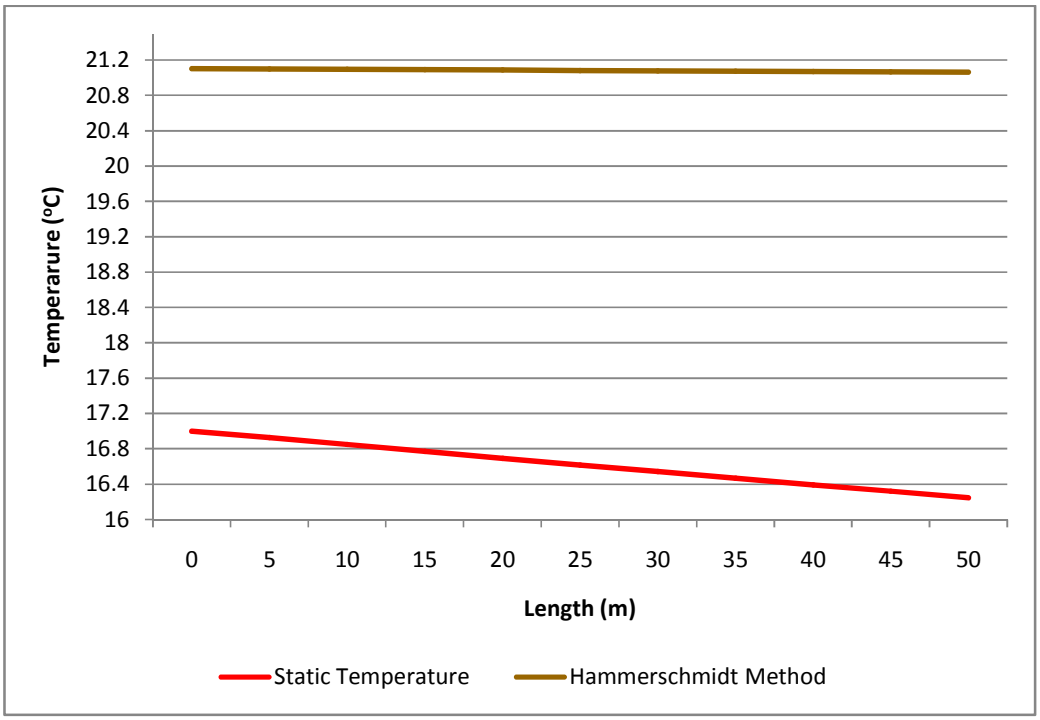

Figure 4.13 Comparison between static temperature of the 2-phase flow and Hammerschmidt Method along 50 meter pipeline

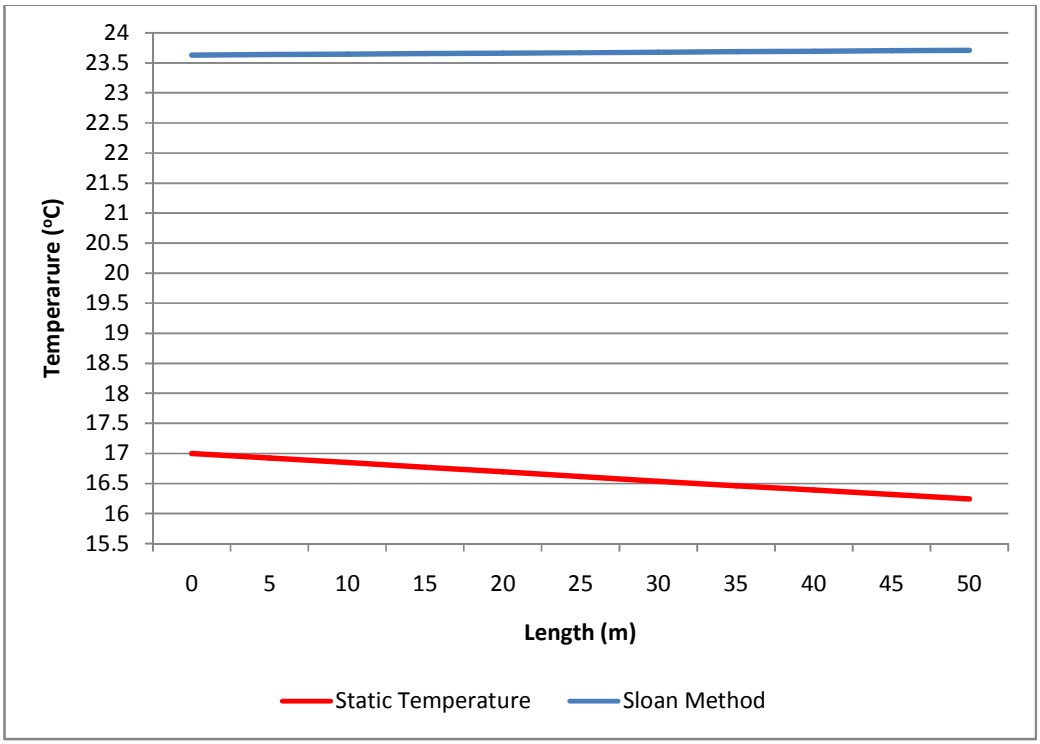

Figure 4.14 Comparison between static temperature of the 2-phase flow and Sloan Method along 50 meter pipeline

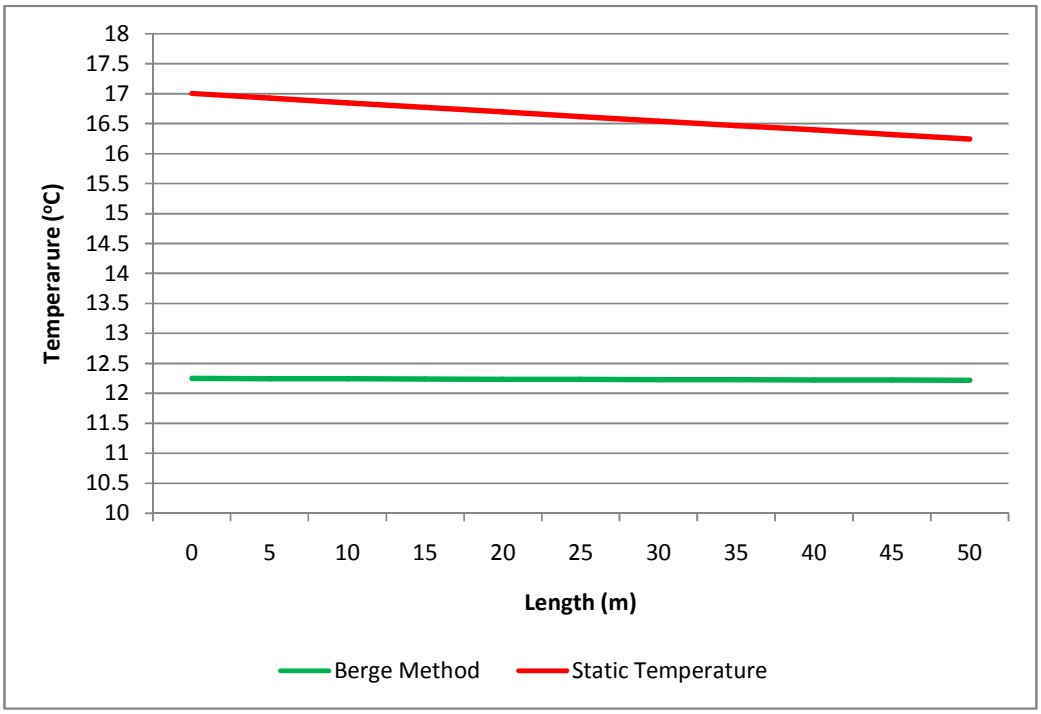

Figure 4.15 Comparison between static temperature of the 2-phase flow and Berge Method along 50 meter pipeline

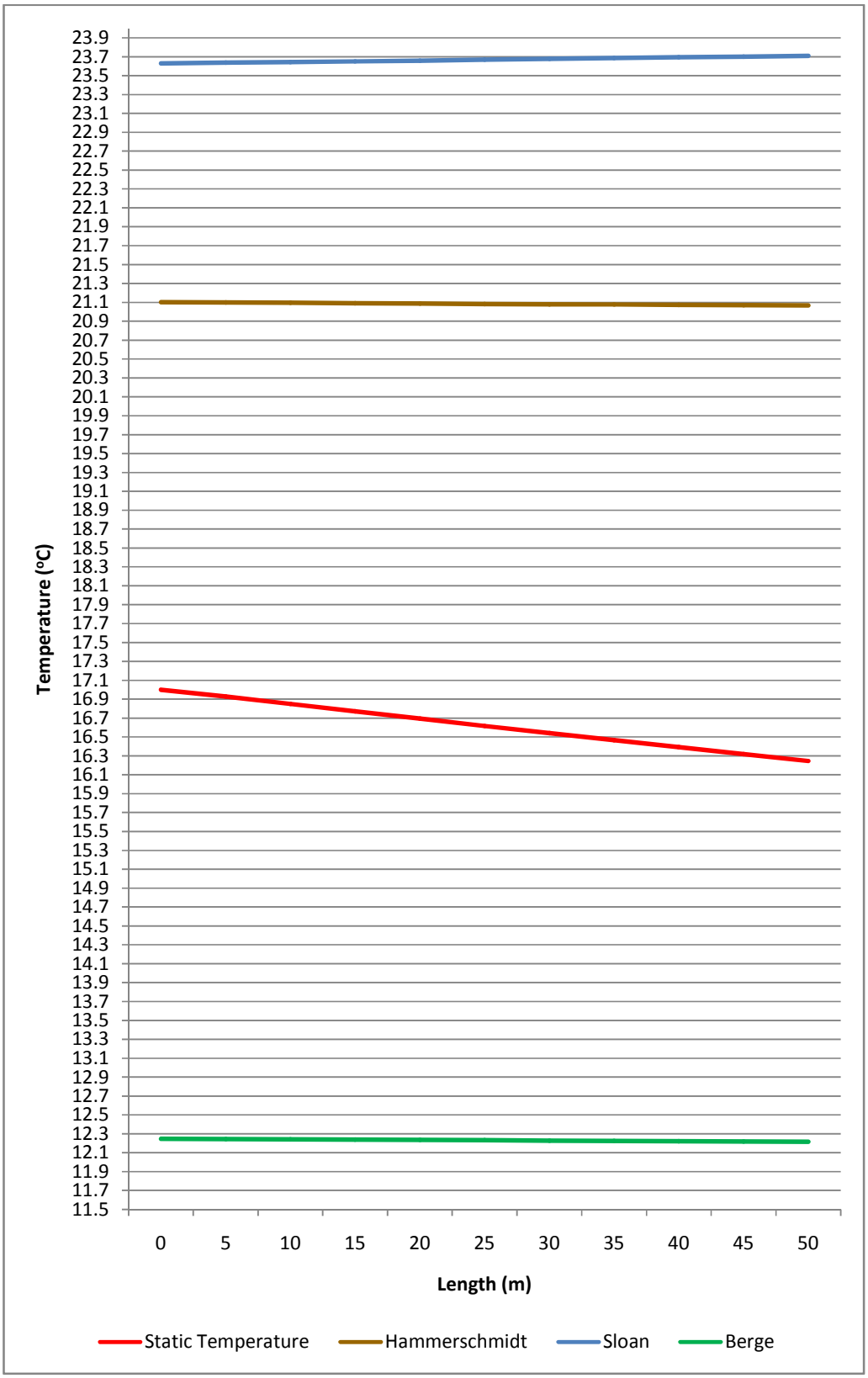

Figure 4.16 Comparison between flow temperature and hydrates formation temperature calculated using various empirical methods along 50 meter pipeline

The results of the empirical correlation methods applied shows that different methods produce different trends of hydrates formation temperature. From the graphs shown in figure 4.13 and figure 4.14, it shows that both Hammerschmidt and Sloan method predicted that hydrates will form when it is operating at 9.59MPa (1390 psi) as the static temperature is below the hydrates formation temperature. From figure 4.15, the graph shows that the static temperature is above the hydrates formation temperature. From here, the Berge method predicted that hydrates will not form. The accuracy of the empirical methods to determine the hydrates temperature formation is vague as they are just quantitatively depends on the pressure and specific gravity from experimental data which is difficult to obtain.

Therefore, so far this simulation project is able to incorporate three different empirical correlations for hydrates temperature formation prediction. Each of the empirical models is able to predict variation in the hydrates formation temperature which is corresponded to the simulated pressure. However, a complete validation of the results requires experimental data which is difficult to obtain.

From the simulation, it is shown this project illustrates the validity of FLUENT as a CFD code for modelling of multiphase flow. Although the input from FLUENT requires value from data, it still requires empirical study on the continuity, momentum and energy equation to produce a simulation which converges faster. There is a major problem where there is little published work available on multiphase flow simulation in FLUENT especially in oil and gas riser pipeline. Hopefully, with later version of FLUENT will incorporate some improvement in the multiphase simulation and prediction of hydrates formation in longer pipeline. This also comes with the greater performance of simulation machine ability.

CHAPTER 5
CONCLUSION AND RECOMMENDATION

Using FLUENT has been a very challenging exercise in its own even though it is a very user friendly package. The problem which has been burdening the author lies not with the software interface itself but the multitude of options, models and inputs that the author has to familiarise with as soon as possible. The empirical calculation need to be done correctly before the usage of Fluent for simulation.

Although there are extensive manuals of FLUENT 6.2 that are available for reference, it is imperative that a user knows why a particular model is chosen over another. There are numerous options to select from, and the selection of the appropriate model will reduce the time spent on running simulations. The desire results which are analysed also depend on the suitability of the model selected.

5.1 Computational Conclusions

Several conclusions can be made about the results of this project:

- The CFD package has been able to simulate the two phase flow in pipeline and predicted the temperature and pressure drop.
- This input for every option in the user interface is best to determine from empirical methods.
- Incorporate the three different hydrates prediction empirical correlations to complete the simulation, where to produce hydrates function temperature.
- The empirical models predicted variation in hydrates temperature corresponding to the simulated pressure.
- The most important gain is the procedures used to calculate the hydrates formation temperature and analyzed of the results.
- To complete the validation of the simulation, it is best to compare with experiment data, however is difficult to obtain.

5.2 Future Work

Some of the suggested work that could be carried out in the future are:

- Further validation of the results of this project should be carried out in order to determine the type of flow in the pipeline. This is done by obtaining experimental data or any real industrial data. Much accurate analysis will be obtained for multiphase pipeline designs and construction.
- CFD modelling should be carried out with computers that have high computational power and memory. The higher the computational power, the better the accuracy and the reliability of the results produced by simulation. It also saves time through faster rate of convergence. Higher memory allocated can allow the modelling to have more fine meshes in longer pipeline.

REFERENCES

[1] Brill, J.P. and Mukherjee, 1999, *Multiphase Flow in Wells, Monograph Volume 17*, SPE, Henry L.Doherty Series.

[2] Pickering, P.F. , Hewitt, G.F., Watson, M.J., Hale, C.P., 1992, *The Prediction of Flow in Production Risers-Truth or Myth?,* Department of Chemical Engieering & Chemical Technogy, Imperial College of Science, Technology & Medicine

[3] Beggs, H. D., and Brill, J. P., 1973, *A Study of Two-Phase Flow in Inclined Pipes*, Trans. AIME, 255, p. 607.

[4] T.K. Amy, F. Gongmin, A.W. Malene. B.T. Mason, 2002, SPE 74657.

[5] Watson, M.J and Hewitt, G.F., 1999, *Pressure effects on the slug-to-churn transition,* Int J. Multiphase Flow, Vol. 138. p 1225-1241.

[6] Anil W.Date, 2005, *Introduction to Computational Fluid Dynamics*, Cambridge.

[7] Sloan, E.D., 1998, *Clathrate Hydrates of Natural Gases,* Marcel Dekker, New York.

[8] R. Masoudi, B. Tohidi, R. Anderson, R.W. Burgass, J. Yang, 2004, *Experimental measurement and thermodynamic modeling of clathrate hydrate equilibria and salt solubility in aqueous ethylene glycol and electrolyte solutions,* Fluid Phase Equilibria, Science Direct.

[9] Khaled Ahmed Abdel Fattah, 2004, *Evaluation of Empirical Correlations for Natural Gas Hydrate Prediction,* Oil and Gas Business Journal.

[10] O. Shoham, Y.Taitel, 1984, *Stratified turbulent-turbulent gas liquid flow in horizontal and inclined pipes*, AIChE J. 30 (2) 377-385.

[11] R.I. Issa, 1998, *Prediction of turbulent, stratified, two-phase flow in inclined pipes and channels*, Int. J. Multiphase Flow 24 (5) 327-337

[12] C.H. Newton, M. Behnia, 1998, *Numerical calculation of turbulent stratified gas-liquid pipe flows*, Int. J. Multiphase Flow 24 (5) 327-337

[13] G. Subhashini, K.D.P. Nigam, 2006, *CFD modeling of flow profile and interfacial phenomenon in two-phase flow in pipes,* ScienceDirect 45, 55-65

[14] T.C. Clayton, 2006, *Multiphase Flow Handbook,* Taylor and Francis Group

[15] S. Ameripour, 2005, *Prediction of Gas-Hydrate Formation Conditions in Production and Surface Facilities,* Master of Science Thesis, Texas A&M University.

[16] Sinnadurai, S.L. 2007, *A Comparison Study of the Pressure Gradient of a Two-Phases Flow in a Pipeline, Empirical Correlations and Computational Fluid Dynamics Method,* B.Sc. Project, Universiti Teknologi Petronas.

[17] Ganesan, T, 2006, *A Comparison Study Between Empirical Correlations and Computational Fluid Dynamics of the Pressure Gradient of a Multi-Phase Flow in a Pipeline,* B.Sc. Project, Universiti Teknologi Petronas.

APPENDICES

APPENDIX A

Multiphase Mixture Model in FLUENT 6.2

Continuity Equation for the Mixture

The continuity equation for the mixture is

$$\frac{\partial}{\partial t}(\rho_m) + \nabla.(\rho_m \vec{v}_m) = 0$$

where $\vec{v}_m$ is the mass-averaged velocity:

$$\vec{v}_m = \frac{\sum_{k=1}^{n} \alpha_k \rho_k \vec{v}_m}{\rho_m}$$

and ρ_m is the mixture density:

$$\rho_m = \sum_{k=1}^{n} \alpha_k \rho_k$$

α_k is the volume fraction of phase *k*.

Momentum Equation for the Mixture

The momentum equation for the mixture can be obtained by summing the individual momentum equations for all phases. It can be expressed as

$$\frac{\partial}{\partial t}(\rho_m \vec{v}_m) + \nabla.(\rho_m \vec{v}_m \vec{v}_m) = -\nabla\rho + \nabla.[\mu_m(\nabla\vec{v}_m + \nabla\vec{v}_m^T)] + \rho_m\vec{g} + \vec{F} + \nabla.\left(\sum_{k=1}^{n} \alpha_k \rho_k \vec{v}_{dr,k} \vec{v}_{dr,k}\right)$$

Where *n* is the number of phases, $\vec{F}$ is a body force, and μ_m is the viscosity of the mixture:

$$\mu_m = \sum_{k=1}^{n} \alpha_k \mu_k$$

$\vec{v}_{dr,k}$ is the drift velocity for secondary phase k:

$$\vec{v}_{dr,k} = \vec{v}_k - \vec{v}_m$$

Energy Equation for the Mixture

The energy equation for the mixture takes the following form:

$$\frac{\partial}{\partial t}\sum_{k=1}^{n}(\alpha_k \rho_k E_k) + \nabla.\sum_{k=1}^{n}\left(\alpha_k \vec{v}_k(\rho_k E_k + p)\right) = \nabla.\left(k_{eff}\nabla T\right) + S_E$$

where k_{eff} is the effective conductivity ($\sum \alpha_k(k_k + k_t)$), where k_t is the turbulent thermal conductivity, defined according to the turbulence model being used). The first term on the right-hand side represents energy transfer due to conduction. S_E includes any volumetric heat sources.

In the equation above

$$E_k = h_k - \frac{p}{\rho_k} + \frac{v_k^2}{2}$$

For a compressible phase, and $E_k = h_k$ for an incompressible phase, where h_k is the sensible enthalpy for phase *k*.

APPENDIX B

Volume of Fluid (VOF) Model in FLUENT 6.2

The VOF formulation relies on the fact that two or more fluids (or phases) are not interpenetrating. For each additional phase that is added to a model, a variable is introduced: the volume fraction of the phase in the computational cell. In each control volume, the volume fractions of all phases sum to unity. The fields for all variables and properties are shared by the phases and represent volume-averaged values, as long as the volume fraction of each of the phases is known at each location. Thus the variables and properties in any given cell are either purely representative of one of the phases, or representative of a mixture of the phases, depending upon the volume fraction values. In other words, if the *q*th fluid's volume fraction in the cell is denoted as α_q, then the following three conditions are possible:

- $\alpha_q = 0$: the cell is empty (of the *q*th fluid).
- $\alpha_q = 1$: the cell is full (of the *q*th fluid).
- $0 < \alpha_q < 1$: the cell contains the interface between the *q*th fluid and one or more other fluids.

Based on the local value of α_q, the appropriate properties and variables will be assigned to each control volume within the domain.

The Volume Fraction Equation

The tracking of the interface(s) between the phases is accomplished by the solution of a continuity equation for the volume fraction of one (or more) of the phases. For the *q*th phase, this equation has the following form:

$$\frac{1}{\rho_q}\left[\frac{\partial}{\partial t}(\alpha_q \rho_p) + \nabla.(\alpha_q \rho_q \vec{v}_q = S_{\alpha_q} + \sum_{p=1}^{n}(\dot{m}_{pq} - \dot{m}_{qp})\right]$$

Where $\dot{m}_{qp}$ is the mass transfer from phase q to phase p and $\dot{m}_{qp}$ is the mass transfer from phase *p* to phase *q*. The volume fraction equation will now be solved for the

primary phase; the primary-phase volume fraction will be computed based on the following constraint:

$$\sum_{q=1}^{n} \alpha_q = 1$$

Properties

The properties appearing in the transport equations are determined by the presence of the component phases in each control volume. In a two-phase system, the phases are represented by the subscripts 1 and 2, and if the volume fraction of the second of these is being tracked, the density in each cell is given by

$$\rho = \alpha_2 \rho_2 + (1 - \alpha_2)\rho_1$$

In general, for an n-phase system, the volume-fraction-averaged density takes on the following form:

$$\rho = \sum \alpha_q \rho_p$$

All other properties are computed in this manner.

The Momentum Equation

A single momentum equation is solved throughout the domain, and the resulting velocity field is shared among the phases. The momentum equation, shown below, is dependent on the volume fractions of all phases through the properties ρ and μ.

$$\frac{\partial}{\partial x}(\rho \vec{v}) + \nabla.(\rho \vec{v}\vec{v}) = -\nabla p + \nabla.[\mu(\nabla \vec{v} + \nabla \vec{v}^T)] + \rho \vec{g} + \vec{F}$$

One limitation of the shared-fields approximation is that in cases where large velocity differences exist between the phases, the accuracy of the velocities computed near the interface can be adversely affected.

The Energy Equation

The energy equation, also shared among the phases, is shown below.

$$\frac{\partial}{\partial t}(\rho E) + \nabla.\left(\vec{v}(\rho E + \rho)\right) = \nabla.\left(k_{eff}\nabla T\right) + S_h$$

The VOF model treats energy, *E*, and temperature, *T,* as mass-averaged variables:

$$E = \frac{\sum_{q=1}^{n} \alpha_q \rho_q E_q}{\sum_{q=1}^{n} \alpha_q \rho_q}$$

where E_q for each phase is based on the specific heat of that phase and the shared temperature. The properties ρ and k_{eff} (effective thermal conductivity) are shared by the phases. The source term S_h, contains contributions from radiation, as well as any other volumetric heat sources.

As with the velocity field, the accuracy of the temperature near the interface is limited in cases where large temperature differences exist between the phases. Such problems also arise in cases where the properties vary by several orders of magnitude.

APPENDIX C

Phase Diagram of Methane-Water

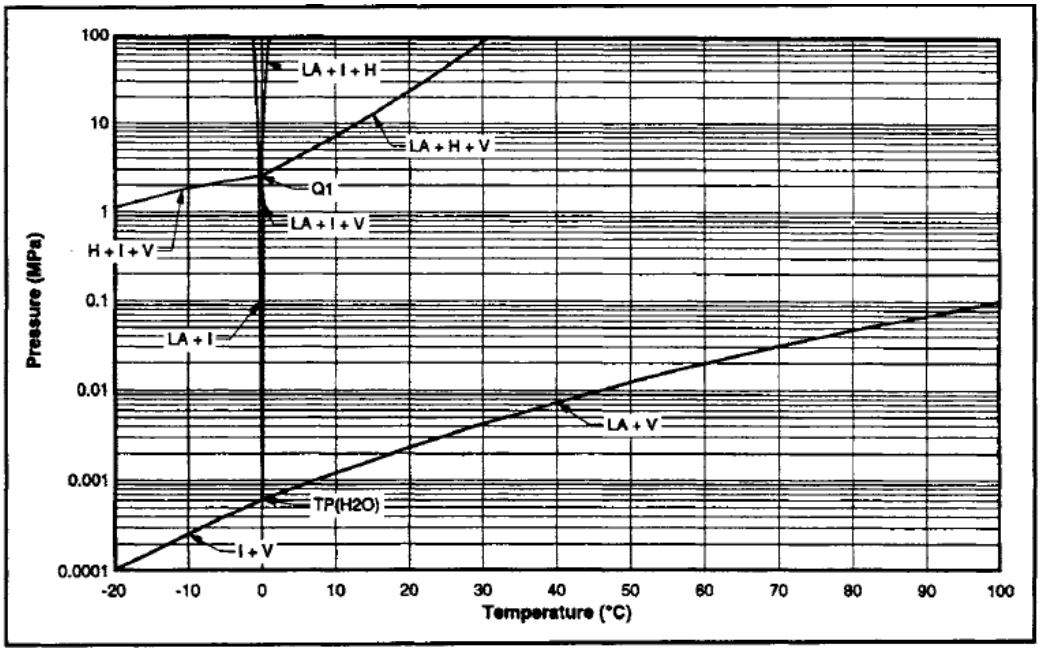

Figure C1 The pressure-temperature diagram for the system methane + water

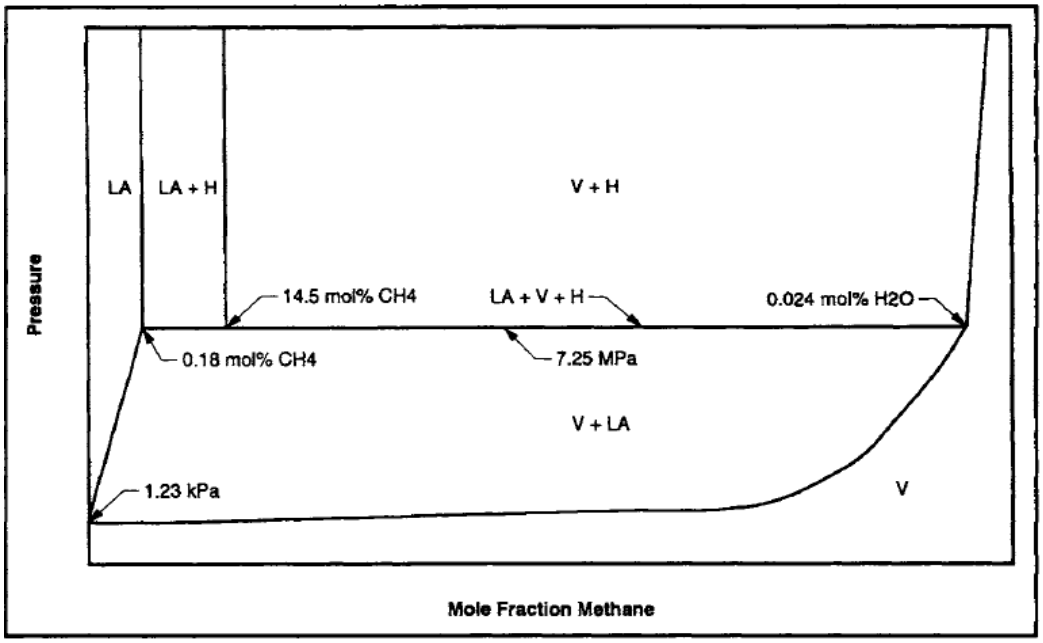

Figure C2 Pressure-composition diagram for methane + water at 10^{o}C (not to scale)

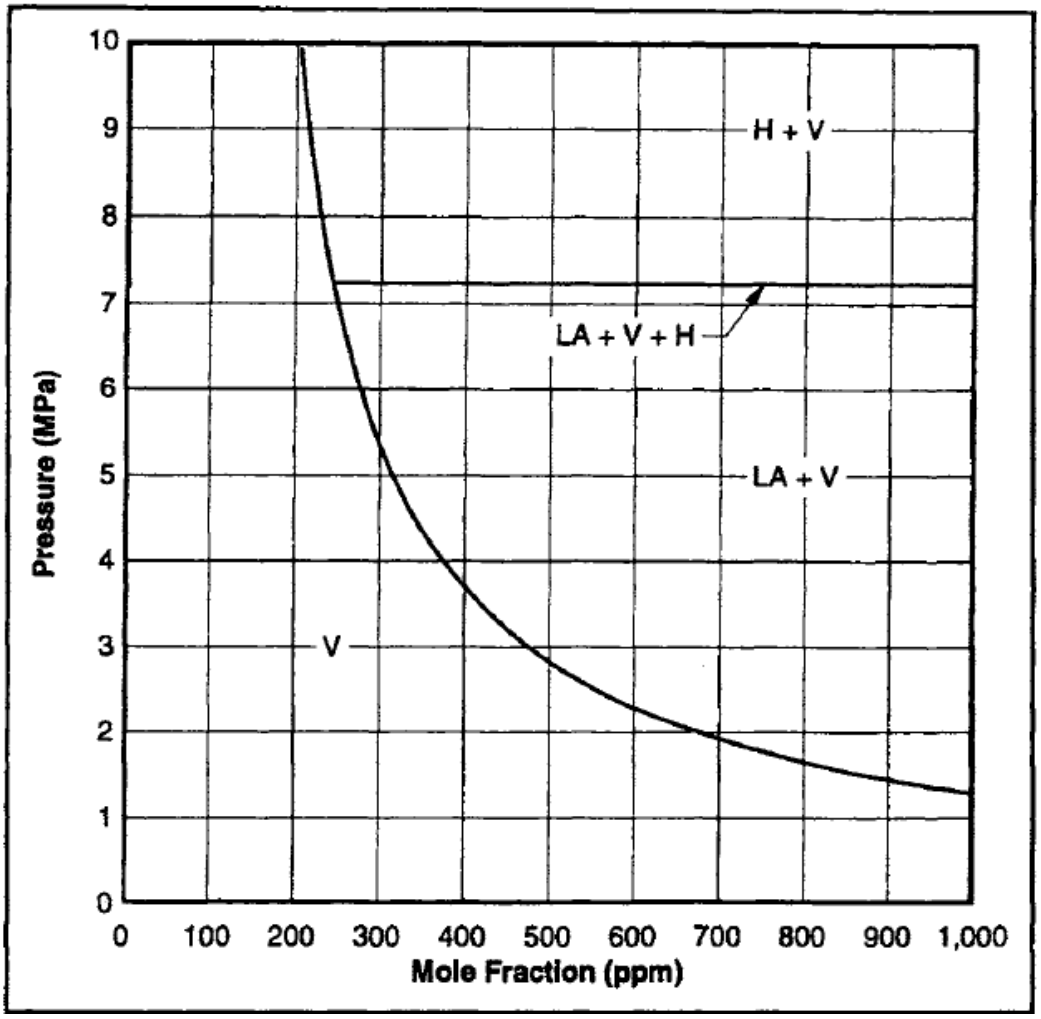

Figure C3 Pressure-composition diagram for methane + water at 10^{o}C (magnified region to scale)

********** END OF REPORT **********